THE FATIGUE OF ORDERED Cu_3Au

THE FATIGUE OF ORDERED Cu_3Au

By

ALISTAIR GORDON YOUNG, A.R.C.S.T.

A Thesis

Submitted to the Faculty of Graduate Studies

in Partial Fulfilment of the Requirements

for the Degree

Master of Science

McMaster University

October 1966

MASTER OF SCIENCE (1966) McMASTER UNIVERSITY
(Metallurgy) Hamilton, Ontario

TITLE: The Fatigue of Ordered Cu_3Au

AUTHOR: Alistair Gordon Young, A.R.C.S.T.

SUPERVISOR: Professor R. K. Ham

NUMBER OF PAGES: vii, 52

SCOPE AND CONTENTS:

Current theories to explain the strengthening caused by ordering are reviewed. Localization of slip was observed to occur during high strain reverse bending, and was associated with crack initiation. A mechanism for the breakdown of order strengthening mechanisms is suggested as an explanation for this localization.

ACKNOWLEDGEMENTS

The author is indebted to Dr. R. K. Ham for his continued encouragement and assistance during the course of this work.

The X-ray work was carried out at the Ontario Research Foundation with the assistance of Mr. E. Niskanen and this is gratefully acknowledged.

This work was supported by the National Research Council of Canada.

TABLE OF CONTENTS

LIST OF FIGURES

LIST OF TABLES

CHAPTER I

INTRODUCTION

In many cases, fatigue crack initiation can be associated with regions of localized slip[1], so that, since a general feature of ordered alloys is that slip remains fine and evenly distributed[2], it might be expected that the fatigue strength of these alloys would be increased above that of their disordered counterparts. Such an effect has been demonstrated by Davies and Stoloff[3] in polycrystalline Ni_3Mn and FeCo, and by Rudolph et al[4] in single crystals of Cu_3Au.

However, for fatigue crack initiation to occur at regions of localized slip, as proposed above, suggests that the process which prevents slip localization in ordered alloys must break down, or, alternatively, a process which causes slip localization must develop.

The purpose of this work was to investigate the damage caused by fatigue of ordered Cu_3Au.

The progress of fatigue deformation was followed by optical microscopy and microhardness measurements. After fatigue, replicas of the surface were taken. Thin film electron microscopy and X-ray intensity measurements were used to determine the changes, caused by fatigue, in the ordered structure of Cu_3Au. Specimens were prepared in the form of thin sheets to facilitate thin film electron microscopy.

CHAPTER II

PREVIOUS WORK

Only three investigations[3,4,5] have been made into the effect of fatigue on ordered alloys. In all cases, tests were conducted at small stress amplitudes. Also, in every case apart from polycrystalline β-brass[5], the slip lines after fatigue were fine and evenly distributed. In the case of polycrystalline β-brass this was the general feature, but slip localization occurred at grain boundaries.

Fatigue crack initiation in ordered Cu_3Au[4] and β-brass[5] single crystals is associated with slip lines. In Ni_3Mn[3], FeCo[3] and β-brass[5] polycrystals there is, apparently, a greater tendency for cracks to nucleate at grain boundaries. This is a common feature in fatigue, and has been attributed to the stress concentrations at grain boundaries[1]. It was suggested that these would give rise to regions of increased slip activity, and hence localized acceleration of the fatigue process. Evidence that this explanation may be applicable, at least in some cases, to ordered polycrystals, is thought to be provided by the observations made on the fatigue of β-brass. Due to a large elastic anisotropy in this alloy, grain boundary stress concentrations are very large[5]. In this case, slip concentration in the vicinity of the grain boundaries was observable, and did, in many cases, cause crack initiation.

Rudolph et al[4] found, from X-ray intensity measurements, that no change in the long range order parameter had been caused by fatigue.

CHAPTER III

THEORY

The equilibrium atomic configuration and dislocation structure in ordered Cu_3Au are described and theories on the effect of these on the strength, and work hardening rate are outlined.

1. Order in Cu_3Au

Long Range and Short Range Order

In a substitutional solid solution the constituent atoms are often more or less randomly arranged on the atomic positions of the lattice of the base metal. However, certain alloys exhibit preferential positioning, or ordering, of the constituent species, such that an atom is surrounded by the maximum number of unlike nearest neighbours, with a consequent decrease in internal energy. The resulting lattice can be described by a sub-lattice of A-atoms, and a sub-lattice of B atoms, combining to form a superlattice. In the case of the Cu_3Au alloy, the perfectly ordered structure consists of four inter-penetrating simple cubic sub-lattices, one of which consists of gold atoms, the other three of which consist of copper atoms, combining to form an f.c.c. structure. The crystal structure of Cu_3Au thus remains unchanged upon ordering, but the symmetry is lower than the parent disordered phase. The latter effect is common to all superlattices and gives rise to extra lines or spots--superlattice reflections--on a diffraction pattern.

Long range order is said to exist when a greater fraction of like atoms than would be expected from consideration of the alloy composition, choose to occupy the same sub-lattice (or set of sub-lattices) throughout the alloy. To measure the extent of this effect, a long range order parameter is defined as

$$S = \frac{p - r}{1 - r}$$

where p is the proportion of A sites filled by A atoms, and r is the proportion of A atoms in the alloy. It has a value of unity when the separation of constituent species onto different sub-lattices is complete, i.e., for perfect long range order, and has a value of zero when all sub-lattices are, on the average, occupied randomly, i.e., for no long range order.

However, very high degrees of order can exist even though the long range order parameter is zero. Bethe[6] has stated that the preference for unlike nearest neighbours always exists in these alloys, and can manifest itself by the formation of small highly ordered groups, which need not have a predominant overall sub-lattice allocation. Thus it is convenient to define a short range order parameter as a measure of the unlike nearest neighbours in excess of that expected from consideration of the alloy composition. This parameter is defined as

$$\alpha_m = 1 - \frac{n_{BA}}{r}$$

where n_{BA} is the proportion of m^{th} nearest neighbours of A to a B atom and r is the proportion of A atoms in the alloy, such that when every atom has all nearest neighbours in the proportions expected from consideration of the composition, $\alpha_{m=1}$ has a value of zero. Non-zero values indicate the presence of short range order but the relation is not simple (see below).

It is obvious that in Cu_3Au, every atom in the alloy cannot have all unlike nearest neighbours, and that there must be a large number of Cu-Cu bonds. In Cu_3Au with perfect long range order, each Au atom has 12 Cu nearest neighbours, while each Cu atom has 4 Au and 8 Cu nearest neighbours. Comparing the latter with the fact that in completely disordered Cu_3Au every atom will have 3 Au and 9 Cu nearest neighbours, it is seen that upon ordering each Cu atom gains only 1 Au nearest neighbour, and not the 9 required for perfect short range order. Guinier[7] shows that by considering first nearest neighbours only, the short range order parameter, as defined above, in perfectly ordered Cu_3Au is -1/3 and that if 2nd nearest neighbours only are considered, the short range order parameter is 1. Successive odd and even orders of nearest neighbours give short range order parameters of -1/3 and 1 respectively, due to the periodicity of the lattice.

Ordering Process

By considering both the fact that Cu_3Au orders by a first order reaction[8], and the thermodynamic relationship

$$\Delta F = \Delta E - T\Delta S \ ,$$

the process by which Cu_3Au orders under equilibrium conditions can be visualized, in terms of configuration.

The temperature must be lower than a critical T_c, where $\Delta E = T_c\Delta S$, before the ordering is thermodynamically stable. However, above this temperature, since there is always a preference for unlike nearest neighbours, small ordered groups form and disperse causing a finite short range

order parameter. Just below T_c, these groups are stable nuclei for highly ordered domains which grow at the expense of disordered material until they coalesce with other domains, if their sub-lattice allocation is the same, or form 'change step' boundaries called anti phase domain boundaries (APDB), if their sub-lattice allocations differ. Further growth of domains is at the expense of other domains, and is slower than would be expected from diffusion considerations, being retarded by the formation of a metastable structure. The details of this metastable structure will be discussed in the next section. Although it was stated that Cu_3Au ordered by a first order reaction, this is not completely true, since the equilibrium degree of long range order rises homogeneously from 0.8 at T_c to 1 with decrease in temperature.

2. Anti Phase Domain Boundaries (APDB)

The first direct observation of APDB's was made in 1958 by Ogawa et al[9], who examined thin films of ordered CuAu by transmission electron microscopy. An excellent review of subsequent electron microscopy of ordered alloys is given by Marcinkowski[10].

Following Marcinkowski, APDB's are distinguished by their plane, and the vector which would move one domain relative to the other such that sub-lattice allocation in the two domains were identical. Since there is a choice of four sub-lattices in Cu_3Au, there are three 'correcting' vectors, and these are of the $1/2\ a_o$ <110> type. These vectors may or may not be on the plane of the APDB, and would signify a shear on the plane, or a displacement of the plane, respectively.

It is helpful in visualizing these APDB types to consider the growth of domains.

When two domains meet, it is possible that the (100) type plane (determined by occupancy) in one domain would meet the (100) type plane, rather than the (200) type plane, in the other domain. The APDB thus formed can be imagined as the removal of a (200) plane from an otherwise ordered lattice, and the gap filled by the displacement of the crystal on one side by a vector 1/2 a_o <110>. This gives rise to an APDB whose vector does not lie on the plane of the APDB, and is known as a 'Type 2' APDB or an APDB 'of the 2nd kind'.

However, should the (100) plane in one domain have met the (200) plane in the other domain, and had the sub-lattice allocation differed, the APDB thus formed could be visualized as a 1/2 a_o <110> shear on the (100) plane. In this case, the vector does lie on the plane of the APDB and these are denoted 'Type 1' or APDB's 'of the 1st kind'.

Electron microscopical observations show domains to be continuous through twin boundaries, and discontinuous at grain boundaries[10]. This would seem to be evidence for a short range ordering interaction. Indeed, Cowley[11] and Sutcliffe and Jaumot[12] have estimated that second nearest neighbour interactions are only 1/10 as strong as first nearest neighbour interactions in Cu_3Au. It is obvious then that the energy of an APDB depends upon its plane and vector, since, in perfectly ordered Cu_3Au, these two specify the nearest neighbour interactions involved, and upon the equilibrium degree of long range order, since a decrease in the latter causes a fewer number of like nearest neighbour bonds to be created, and hence a decrease in the APDB energy.

The (100) planes in perfectly ordered Cu_3Au are 'sandwiched' between (200) planes which consist entirely of copper atoms, and, since all its neighbours are on (200) planes, a (100) APDB of the 1st kind is unique in that no new wrong nearest neighbours are formed. It is, therefore, a very low energy APDB, its energy being due only to wrong second nearest neighbours.

However, by removing a (100) plane to produce a (200) APDB of the 2nd kind, two planes of Cu atoms come in contact, producing a high energy APDB.

It is expected that high energy APDB's are the driving force for domain growth, while the low energy (100) type 1 APDB's retard growth. Thus in a well-annealed structure it would be expected that the majority of APDB's would lie on (100) planes.

This is borne out by electron microscopy observations. However, a 'maze pattern' rather than a complete network of APDB's is observed, since contrast conditions will not usually be such that all APDB's are revealed simultaneously. It is noteworthy that even under conditions which would reveal a complete network of (100) APDB's of the 1st kind, this is not observed, suggesting that such a low energy configuration is never obtained.

3. Superdislocations

The fact that the motion of an ordinary dislocation in an ordered structure will create a sheet of APDB was first recognized by Koehler and Seitz[13]. To minimize the extra energy so produced, such a dislocation will be followed by one or more identical dislocations such that the order is restored. This group is known as a 'superdislocation'.

Specifically, in Cu_3Au, a superdislocation consists of a pair of ordinary 1/2 a_o <110> dislocations separated by a 1/2 a_o <110> APDB of the 1st kind. It should be noted that all APDB's created by dislocations must be of this shear type.

The smaller the separation of the pairs, the less APDB is created, but the greater is the repulsive elastic interaction between the dislocations. Thus an equilibrium separation is associated with the plane of the APDB being created, and the degree of long range order present, since these determine the APDB energy; together with the type of dislocation, since screws have a smaller repulsive interaction than edges. For example, on the (111) plane in highly ordered Cu_3Au, Kear[14] observed the separation of two screw dislocations to be approximately 140 Å, and the separation of two edges to be approximately 200 Å; whereas on the (100) plane, the separation of two screws was approximately 450 Å.

It is expected in f.c.c. that the dislocations will be extended, and Marcinkowski and Miller[15] have suggested that the stacking fault energy will be increased in an ordered material, thus decreasing the separation of the partials. However, although this effect has been observed in Ni_3Mn[15], Marcinkowski and Zwell[16] observed the opposite effect in Cu_3Au and concluded that the stacking fault energy in Cu_3Au is, in fact, lowered. X-ray analyses[17,18] have led to the same conclusion.

4. Order Hardening

To isolate the effect of order on strength it is necessary to have a constant domain size. Fortunately, in Cu_3Au, as was mentioned, domain growth becomes very sluggish after a time. Thus it is assumed that,

allowing sufficient time, an equilibrium domain size is obtained, and that the increase of the long range order parameter which is observed on decreasing the temperature is due only to rearrangement of atoms within the domains.

Experiments carried out on this basis are of two types: those testing specimens at the temperature, and those testing specimens quenched from the temperature, at which they were equilibrated.

Ardley[19] showed, from tests carried out at temperature, that decreasing the long range order parameter, by increasing the temperature, caused an increase in strength. At T_c, there was a drop in strength as the order changed from a long range order of 0.8 to short range order. Further increase in temperature, or decrease in short range order, was observed to raise the strength again. These observations are shown in Fig. 1.

To explain the results below T_c, Ardley extended Fisher's[20] short range order hardening mechanism to apply to long range order. Basically Fisher's theory says that since a unit dislocation does not recreate the atomic configuration through which it passes, it will destroy short range order across its slip plane. This causes an increase in internal energy so that to pass a unit dislocation through short range order requires a higher applied stress than that to pass one through a completely disordered material. It was considerations of this type that led to the theory of superdislocations in long range ordered materials, since these would recreate the atomic configuration. However, Ardley suggests that in less than perfect long range order, a superdislocation will not recreate the atomic configuration, and will cause disordering, thus explaining the

observed increase in strength with decrease in long range order. Davies and Stoloff[21] have pointed out that although superdislocations would not recreate the initial atomic configuration, on average they would be expected to correct as many wrong bonds as they destroyed.

To explain the maximum in strength with change in temperature, Davies and Stoloff[21] used an idea first proposed by Marcinkowski et al[22,15] to explain similar behaviour in Ni_3Mn. Although Ni_3Mn forms the same superlattice as Cu_3Au, it differs from Cu_3Au in that short range order is stable below T_c, the order increasing by an increase in the proportion of long range ordered to short range ordered material with decrease in temperature. Marcinkowski et al drew attention to the fact that the width of superdislocations depends upon the degree of order, so that superdislocations would meet resistance in short range ordered material. Davies and Stoloff extended this idea to form a universal theory by saying that, if the degree of long range order was sufficiently low, unit dislocations would predominate and strength would increase with an increase in order by Fisher's mechanism; while, if the degree of long range order was high, superdislocations would predominate and strength would decrease with increase in order, due to the decreasing proportion of unit dislocations. Thus a maximum at an intermediate degree of long range order would be expected, corresponding to the transition from a predominance of unit dislocations to a predominance of superdislocations. Cu_3Au, they explained, is a special case since the transition in this alloy would be expected at T_c as, above this temperature long range order is non-existent, while below this temperature short range order is non-existent. However, their explanation that the increase in strength of Cu_3Au, when the long range

order parameter changes from 1 to 0.8, is due to an increase in the probability of dissociation of superdislocations would seem to be rather a fine point when it is considered that unit dislocations would be unstable in this alloy under the conditions considered. The equilibrium width of superdislocations in perfectly ordered Cu_3Au is approximately 130 Å[10], and since the width is inversely proportional to the square of the long range order parameter[10], the equilibrium separation at 0.8 should be approximately 200 Å.

The specimens Ardley tested above T_c exhibited yield points, an inverse rate effect (a decrease in strength with increase in strain rate) and discontinuous yielding at a constant average stress similar to that caused by Lüders band propagation. Ardley suggests that these observations are consistent with a strain ageing effect which, he explains, could be due to any or all of Cottrell locking, Suzuki pinning, and Fisher hardening. The increase in strength with increase in temperature is associated with an increase in diffusion rates which, Ardley suggests, would allow a greater amount of strain ageing to occur simultaneously with deformation. Theories[15,19,21,23] concerned with the effect above T_c, whether explaining tests at temperature, as does Ardley's, or explaining tests on quenched specimens, are invariably based on Fisher's short range order hardening theory. While this may be applicable to many alloys, its aptness to Cu_3Au seems doubtful in the light of experiments carried out by Kuczynski, Doyama and Fine[24]. In these tests, the Cu_3Au polycrystalline specimens were equilibrated at temperatures above and below T_c, but, in contrast to Ardley's experiment, they were then quenched and tested at room temperature. Similar to Ardley's results, strength increases with

decrease in order, whether short or long range; however, in contrast to Ardley, the strength rises suddenly at T_c as the order changes from a long range order parameter of 0.8 to short range order. These results are shown in Fig. 2. Using Fisher's theory to explain behaviour above T_c, it would be expected, since diffusion is no longer a variable, that the strength would decrease with increasing quench temperature due to the resulting decrease in short range order.

It should be added that while Sumino[23] agrees that Fisher's mechanism should be predominant above T_c, he suggests that short range order will have an additional effect. This is a locking mechanism due to the interaction of the stress field of a dislocation with the strain field caused by the lattice parameter change on ordering. This strain field should exist when there is a mixture of short range order and long range order or disordered material. Thus an increase in strength with decrease in temperature to T_c would be expected with Cu_3Au due to the increasing amounts of short range order in disordered material. Below T_c the effect should not apply due to the absence of short range order. So that, even neglecting the fact that the lattice parameter change on ordering Cu_3Au is small, the results of Kuczynski et al are inconsistent with this theory.

The cross-slip pinning mechanism[14,25] is now extended to explain the observed strengthening of long range ordered Cu_3Au as its order decreases.

There is evidence[3,4,14,25] that the frequency of cross-slip in Cu_3Au decreases with increase in the degree of long range order. This can be explained by consideration of the energy required to constrict the leading extended dislocation of a pure screw superdislocation, a process

which must take place before cross-slip can occur. A decrease in the degree of long range order causes an increase in the stacking fault energy in Cu_3Au and, hence, a decrease in the separation of the partials[16]. Thus the activation energy required for cross-slip must decrease with decrease in the degree of long range order, and cause an increase in the frequency of cross-slip.

Since (100) type 1 APDB's have an extremely low energy[26], it is expected that superdislocations which cross-slip onto these planes would be virtually pinned[14,25]. Thus it is postulated that the strengthening of long range ordered Cu_3Au with decrease in order is due to an increase in the frequency of cross-slip, and hence an increase in the pinning of superdislocations on (100) planes. This strengthening effect cannot be as great as the strengthening mechanism operating in the short range ordered material, if the increase in strength as long range order changes from 0.8 to 0, as observed by Kuszynski et al[24], is to be explained. These workers showed that as the long range order begins to decrease rapidly to 0.8, the yield strength increases, but the work hardening rate decreases. This is interpreted as a decrease in effectiveness of pinning at higher stresses, rather than a decrease in effectiveness of pinning with decrease in long range order.

Conducting the tests at temperature should increase the ease of cross-slip, due to thermal activation, at all degrees of long range order, but more so at higher temperatures, the latter corresponding to lower degrees of long range order. Thus the strengthening effect with decrease in degree of long range order is accentuated when tests are carried out

at temperature, and it is postulated that this increase in strength is sufficient to account for the observed increase in strength of long range ordered over short range ordered material, observed in tests carried out at temperature.

Tests at temperature are complicated by the possibility of a decrease in effectiveness of this cross-slip pinning mechanism due to thermal activation, as suggested by Davies and Stoloff[27]. Isolating the effect of temperature, by using perfectly long range ordered material, these workers showed that an increase of temperature from 77 - 250°K caused little change in the yield strength (Fig. 3). Normally the flow stress of an f.c.c. alloy would be expected to decrease with increase in temperature, as in fact does occur with disordered Cu_3Au. It was pointed out by these workers that this, and the increase in work hardening rate of ordered Cu_3Au with temperature, indicated a strengthening mechanism which increased in effectiveness with temperature. The mechanism proposed was the cross-slip pinning mechanism being considered here. However, they noted that in the range 250 - 500°K the work hardening rate decreased again (Fig. 4), and suggested that this meant the effectiveness of this mechanism had been reduced due to thermal activation. It is now suggested that such an assumption would require a knowledge of the effect of temperature on yield stress in this temperature range. This is so since an increase in yield stress, caused by an increase in the frequency of cross-slip, could also decrease the work hardening rate, due to a decrease in the effectiveness of this pinning mechanism at this higher stress. If the latter is the case, the decrease in work hardening rate would indicate, instead, an increase in the effectiveness of this pinning mechanism. Thus it is assumed here, in

the absence of other data, that an increase in temperature does increase the frequency of cross-slip pinning, as indicated by available yield stress data. It is of interest, in this respect, to note that Ardley's results show a c.r.s.s. of $\sim$4.5 kg/mm^2 at 300°C which, by Warren and Keating[28], corresponds to an equilibrium degree of long range order of 0.945; while the room temperature c.r.s.s. of Cu_3Au with a long range order parameter of 0.95 is shown to be $\sim$2 kg/mm^2, i.e., an increase in c.r.s.s. of more than 100% on increasing the temperature from room temperature to 300°C.

5. Domain Hardening

To isolate the effect of APDB size on strength, it is necessary to maintain a constant degree of long range order within the domains, and for this reason domain hardening is studied during isothermal annealing below T_c.

A maximum in the yield strength[19,29], and in the hardness[30] of Cu_3Au occurs at a domain size of 30 - 40Å. The hardness vs. domain size results quoted are shown in Fig. 5.

Davies and Stoloff[30] determined both the degree of long range order and the domain size of the specimens tested. These results are shown in Fig. 6.

It is seen that the critical domain size, with respect to strengthening, corresponds to a long range order parameter of less than the equilibrium value. Since Cu_3Au orders by nucleation and growth of nearly perfectly ordered domains, a degree of long range order less than the equilibrium value is indicative of the existence of short range order. Thus the maximum in strength occurs when the two phases, long range order and short

range order, co-exist. Since it is expected that deformation is by unit dislocations in short range order, and by superdislocations in long range order, Davies and Stoloff suggest that the peak in hardness corresponds to a transition between deformation by unit dislocations and deformation by superdislocations. Their theory, which was outlined in the previous section, is that hardening is due to the resistance that unit dislocations will meet in long range order, as opposed to a similar theory[22] which proposed that hardening is due to the resistance that superdislocations would meet in short range order. Thus, by Davies and Stoloff, the maximum in strength corresponds to the greatest amount of ordered material consistent with deformation by unit dislocations, and that the subsequent decrease in strength is due to increasing deformation by superdislocations.

However, it is seen from comparison of Figs. 5 and 6 that even when short range order is absent (corresponding to domain size 100 Å) the hardness continues to decrease with increase in domain size. Davies and Stoloff suggest that this is due to a mechanism originally proposed by Cottrell[31] to explain the maximum in strength in Cu_3Au. Cottrell drew attention to the fact that although superdislocations will not create APDB within a domain, they will jog the APDB's between domains, thus increasing the internal energy and hence applied stress. Thus the strength of Cu_3Au will depend on the frequency with which a superdislocation will meet an APDB, i.e., on the domain size, such that with increase in domain size the strength of Cu_3Au decreases.

6. Work Hardening

The work hardening rate of ordered Cu_3Au is a function of the degree of long range order, domain size, and temperature. The effect of the degree of order and temperature have been shown to differ qualitatively for single and polycrystals. However, no work has been done on the variation of the rate of work hardening with domain size in single crystals.

The rate of work hardening increases with degree of long range order in single crystals[32]; however, it has been shown that this is so in polycrystals until the very final stages of order, whereupon the work hardening rate decreases an equivalent amount[24]. The effect of increase in domain size in polycrystals is small, but does cause an increase in the rate of work hardening[33]. At 77°K the work hardening rates of ordered and disordered single crystals are approximately the same[27]. With increase in temperature from 77 to 350°K, the rate of work hardening of ordered single crystals increases, while that for disordered single crystals slightly decreases. Above 350°K, the work hardening rate of the ordered crystals decreases until, at ~500°K, the rate is the same as at 77°K. The work hardening rate of ordered polycrystalline Cu_3Au appears to be little affected by temperature[34].

There is a characteristic distinction between the slip appearance of deformed, ordered and disordered materials. Whereas slip in disordered material localizes to form distinct slip bands, the slip in ordered material is fine and evenly distributed.[2]

Slip is on {111} planes and in [110] directions in both ordered and disordered material[7]. As a result of X-ray rotation studies on

ordered single crystals[14], it was suggested that in stage II, the rapid work hardening stage, only primary slip occurs. Recently, however, small localized regions of secondary slip have been observed in thin films of specimens deformed in stage II[41]. Electron microscopy has revealed that the majority of dislocations in ordered single[14] and polycrystals[35] are long straight screws with their connecting APDB apparently lying on {100} planes. X-ray studies[17,34] and electron microscopy[34,35] of ordered polycrystals, and electron microscopy[14] of single crystals have revealed that (100) and (111) APDB's are produced by deformation, the relative amounts depending on temperature[34].

Theories which could contribute to the explanation of these observations will now be discussed.

The first work hardening theory for ordered alloys, proposed by Flinn[26], attempted to explain the observation that the rate of work hardening for polycrystalline materials in the ordered condition was greater than that for the corresponding disordered material. Flinn argued that since a superdislocation produces APDB on its slip plane, as suggested by Cottrell[31], the amount of boundary encountered by a superdislocation moving on an intersecting slip plane would be increased, thus causing an increase in the flow stress, and hence work hardening rate.

Flinn proposed a mechanism based on the climb of dislocations onto (100) planes to explain the temperature dependence of the work hardening rate of ordered alloys, but suggested that it would not be applicable to Cu_3Au since the diffusion rates in this alloy would be too low for climb, even at T_c.

The characteristic difference in slip appearance--coarse and localized slip in disordered materials; fine and regular slip in ordered materials--was explained by Flinn as follows.

It is expected that the 'disordered' material will contain short range order, and, since a unit dislocation passing through short range order will disorder its slip plane[20], subsequent slip will be easier on this plane, thus giving rise to the characteristic coarse, localized slip. This explanation has been generally accepted.

In the ordered alloy, the resistance to slip will not be removed by the passage of a superdislocation since, as Flinn pointed out, a superdislocation on an already slipped plane will still create the same amount of APDB on cutting a domain boundary. Since there is no tendency for localization of slip, Flinn suggests, therefore, that the slip should be fine and evenly spaced. It could be further suggested that the friction stress is actually larger on a superdislocation moving on an already slipped plane, thus providing a definite incentive for slip on other planes. This is argued as follows: the first superdislocation to move will create APDB on its slip plane at every domain boundary it meets. The displacement vector of the APDB produced by the passage of this superdislocation will be that of the original boundary. Considering the typical grown-in domain structure of Cu_3Au, i.e., (100) shear APDB, it is seen that there are two possible 1/2 a_o <110> shear vectors for each (100) plane, but that both of these give identical final configurations. Thus any (111) plane passing through a (100) APDB will have one slip vector which is the same as the displacement vector of the grown-in (100) APDB and will, therefore, correct any slip-produced APDB at this boundary. However, the other two

possible slip vectors on the (111) plane will not correct this APDB. Consider the motion of a superdislocation whose unit dislocations do not have the same Burgers vector as the (100) APDB, and hence will not correct the APDB created on the slip plane at this boundary by previous slip. Since neither unit dislocation can correct this APDB, they both will meet, and leave disorder in this region, so that the resistance to their passage should be due only to the extension of the APDB on the (111) plane.

Consider now the motion of a superdislocation where unit dislocations have the same displacement vector as the APDB. The roles of the unit dislocations comprising this superdislocation will be interchanged when they meet the new APDB. This is so since the leading unit will correct the APDB, while the following unit will create APDB again. The first unit will be pulled into the APDB to correct it, thus the region between the two units will now be partly ordered and partly disordered. Once the following unit meets this ordered portion, further motion will require that both unit dislocations create APDB. Thus the leading unit must create an excess of APDB as a driving force before the following unit will move through the ordered region. This friction force will increase with amount of previous slip on the plane. Since a specific superdislocation will have the same (or equivalent) displacement vector as one of the three (100) APDB types it will meet, it is suggested that on average 1/3 of the APDB's encountered by a superdislocation in Cu_3Au will give rise to the friction force outlined above.

Vidoz and Brown[36] and Pampillo[40] suggest that Flinn's mechanism would predict a work hardening rate which decreases with increase in the

original domain size, such that at very large domain sizes its contribution to work hardening would be small. The fact that the work hardening rate of ordered material with very large domain sizes is greater than that for disordered material prompted Vidoz and Brown to propose a contribution to work hardening, complementary to Flinn's, which was independent of the original domain size.

The mechanism of Vidoz and Brown proposed as a contribution to work hardening is based on the jog theory of work hardening[37]. However, they suggest that the effect of ordering would be to cause an additional contribution to the dragging force of jogs. Their argument is that a jog in a superdislocation will not usually be aligned such that the APDB created by the jog on the leading unit is corrected by the jog on the following unit. The result of such a misalignment will be that a tube of APDB will be created when the jog on the superdislocation moves, hence requiring an increase in the applied stress. An increase in the jog density with strain will cause the work hardening rate. It was suggested that at low strains the jog density would be too low for this mechanism to be important, and therefore in the early stages of work hardening, it was proposed, Flinn's mechanism would be the main source of hardening.

Using single crystals of ordered and disordered Cu_3Au, Kear[14] showed that, similar to polycrystals, the work hardening rate for the ordered single crystals was higher than that for the disordered crystals. However, in contrast to the deformation of polycrystals, for which intersecting slip is necessitated, X-ray crystal rotation analyses of ordered single crystals suggested that no intersecting slip had occurred during

the rapid work hardening stage, stage II. However, a significant increase in the friction stress on dislocations in stage II in the ordered alloy was noted and attributed to the jog mechanism.

Kear[41] has recently published electron microscopical observations of stage II work hardening in ordered Cu_3Au and he observed that although the X-ray rotation analyses are consistent with slip only on the primary system, secondary slip does, in fact, occur. Slip on the secondary system was localized, but increased in amount with increase in strain. To explain the X-ray rotation data, it was assumed that the total amount of secondary slip, at any stage, must be small compared to that on the primary system. Kear frequently observed dislocation dipoles, and APDB trails which he suggested were consistent with the jog theory of work hardening as proposed by Vidoz and Brown. The observation that slip had occurred mainly on the primary slip planes is not necessarily inconsistent with the jog mechanism since jogs will be formed when the dislocations on the primary planes cut through grown-in forest dislocations. It was stated in the Vidoz and Brown theory that if the grown-in dislocation remained stationary during the cutting process, no APDB would, in some cases, be produced by the subsequent motion of the primary superdislocation. This is so since the leading and following units comprising the superdislocation would be jogged in identical positions such that the line connecting the jogs would be the direction of motion of the superdislocation, and thus the following jog would correct the APDB created by the leading jog. However, it was suggested that the leading unit would usually displace the grown-in dislocation, so that the jogs would then be misaligned, and an APDB tube would be created.

It was also noted that even if the forest dislocation was stationary, the jogs produced may move along the dislocation as it moves, so that

an APDB tube would be created due to this misalignment. However, this is hard to understand, since it suggests that the same jogs formed at the the same forest dislocation would be expected to follow different paths depending on whether they were on the leading or following unit, even though, by following the leading jog, the following jog could restore order.

The suggestion by Vidoz and Brown that the contribution to the work hardening rate proposed by Flinn should be important in the early stages of work hardening seems questionable in the light of Kear's observation that slip occurred predominantly on the primary system especially in these early stages.

Recent work[33] has shown, although the effect seems to be small, that the work hardening rate actually increases with increase in original domain size, in contrast to Flinn's prediction. Pampillo[40] has re-examined the Vidoz and Brown jog theory, and suggested that the effectiveness of this mechanism should depend on the original domain size. He argues that since the amount of slip-produced APDB on the primary planes will depend on the original domain size, then the hardening of the secondary slip systems will increase with decrease in original domain size. So that, the greater the original domain size, the easier secondary slip will be, and hence the more will occur, and the greater will be the work hardening rate by the jog mechanism.

Onset of stage III, corresponding to a decrease in the work hardening rate, was observed by Kear[14] to be coincident with the onset of widespread secondary slip. Since the jog mechanism should be important when slip occurs on intersecting systems, this observation might appear to be inconsistent with the jog mechanism. However, Vidoz[38] has explained

it as follows. He suggests that the large amounts of deformation which occurred in stage II will disorder the primary slip planes. The intersecting superdislocations observed in stage III will, therefore, encounter a highly disordered structure, so that Vidoz feels that it is reasonable to expect that the work hardening rate caused by the jog mechanism in stage III would be low.

The last two proposals, viz., that by Vidoz, and that by Pampillo, may appear to be contradictory. Pampillo suggests that the more APDB a superdislocation meets, the more resistance there is to its passage; while Vidoz suggests that the more APDB a superdislocation meets, the easier will be its passage. For both proposals to be correct the resistance offered by an increasing amount of APDB must first increase and finally decrease. Such an effect has been suggested by Cottrell[31] as follows. For large domain sizes, the stress required to produce a certain amount of slip will increase with decrease in domain size, since every superdislocation will create more APDB. At very small domain sizes, however, by assuming a similar number of mobile dislocations are present as are at large domain sizes, it will be seen that only a small amount of slip is required to disorder the slip plane. Thus by assuming that all superdislocations create approximately the same amount of APDB, viz., each creates APDB in some domains, while other domains it meets are already disordered; then on average the amount of APDB created by each dislocation, and hence the resistance to their flow, decreases with decrease in domain size.

The Vidoz and Brown mechanism has been criticized by Davies and Stoloff[27], on the basis of the temperature dependence of the work hardening rate of ordered single crystals.

By the Vidoz and Brown theory, any change in the difference in flow stress between ordered and disordered material is a function of the jog density, elastic constant (G), and the Burgers vector (b). Thus any large difference in the temperature dependence of the work hardening rate of ordered and disordered material must be due to a difference in the rate of jog production and/or a change in the effectiveness of jog pinning due to thermal activation. Vidoz and Brown suggest that it would be unlikely that thermal activation would be large enough to assist the motion of jogs in superdislocations, since this would require the removal of APDB. However, it is expected that thermal activation would assist jog motion in the disordered alloy.

It has been shown that the work hardening rate of ordered polycrystals does not vary significantly with temperature[34]. For the Vidoz and Brown theory to explain this requires, since there is no change in the effectiveness of jog pinning, that the rate of jog production in ordered polycrystals be constant with change in temperature.

Davies and Stoloff[27] have since shown that, with increase in temperature from 77 to 300°K, the work hardening rate of ordered single crystals increased continuously, whereas that for disordered crystals was almost independent of temperature, in this temperature range. They therefore suggested that since Vidoz and Brown had predicted no temperature dependence, their results were inconsistent with the jog theory.

Vidoz and Brown, however, predicted no temperature dependence for the work hardening rate in ordered polycrystals, in which intersecting slip is necessitated, and it would not be surprising if the temperature dependence was different for the stage II work hardening rate in ordered single crystals where it has been shown that primary slip is predominant.

To explain the results of Davies and Stoloff by the jog mechanism, an increase in the rate of production of jogs with temperature would have to occur during stage II. The work hardening rate in the disordered crystal would then remain constant with change in temperature, if the rate of increase of the production of jogs was balanced by a decrease in the effectiveness of pinning due to thermal activation. In the ordered alloy, since thermal activation of jog motion is not expected, the work hardening rate should increase with increase in temperature, due to the corresponding increase in the rate of production of jogs.

Electron microscopy[14,34,35] and X-ray data[17,34] have shown that (111) APDB and (100) APDB are produced by deformation of ordered Cu_3Au. Electron microscopy of specimens from stage II showed dislocations to be mostly screw, i.e., suggesting deformation by edge dislocations, and that the majority of these screw dislocations had their connecting APDB apparently lying on (100) planes[14]. To explain these observations, Kear[14] proposed a work hardening mechanism whereby screw dislocations cross-slip on (100) planes to decrease their APDB energy, and are thus pinned. Subsequent deformation occurs at a higher flow stress since the unpinned edge segments must now be bowed out between the pinned screw segments. For an increase in flow stress with increase in strain it is necessary, since the bowing stress is $\sim \frac{Gb}{L}$, that the separation of pinning points, L, decreases with increase in strain. It appears, from a private communication to Davies and Stoloff[21] that Kear has since found little change in L with strain.

Davies and Stoloff[25] suggested that the work hardening rate, at room temperature, of ordered Cu_3Au is similar to that expected for some

By the Vidoz and Brown theory, any change in the difference in flow stress between ordered and disordered material is a function of the jog density, elastic constant (G), and the Burgers vector (b). Thus any large difference in the temperature dependence of the work hardening rate of ordered and disordered material must be due to a difference in the rate of jog production and/or a change in the effectiveness of jog pinning due to thermal activation. Vidoz and Brown suggest that it would be unlikely that thermal activation would be large enough to assist the motion of jogs in superdislocations, since this would require the removal of APDB. However, it is expected that thermal activation would assist jog motion in the disordered alloy.

It has been shown that the work hardening rate of ordered polycrystals does not vary significantly with temperature[34]. For the Vidoz and Brown theory to explain this requires, since there is no change in the effectiveness of jog pinning, that the rate of jog production in ordered polycrystals be constant with change in temperature.

Davies and Stoloff[27] have since shown that, with increase in temperature from 77 to 300°K, the work hardening rate of ordered single crystals increased continuously, whereas that for disordered crystals was almost independent of temperature, in this temperature range. They therefore suggested that since Vidoz and Brown had predicted no temperature dependence, their results were inconsistent with the jog theory.

Vidoz and Brown, however, predicted no temperature dependence for the work hardening rate in ordered polycrystals, in which intersecting slip is necessitated, and it would not be surprising if the temperature dependence was different for the stage II work hardening rate in ordered single crystals where it has been shown that primary slip is predominant.

To explain the results of Davies and Stoloff by the jog mechanism, an increase in the rate of production of jogs with temperature would have to occur during stage II. The work hardening rate in the disordered crystal would then remain constant with change in temperature, if the rate of increase of the production of jogs was balanced by a decrease in the effectiveness of pinning due to thermal activation. In the ordered alloy, since thermal activation of jog motion is not expected, the work hardening rate should increase with increase in temperature, due to the corresponding increase in the rate of production of jogs.

Electron microscopy[14,34,35] and X-ray data[17,34] have shown that (111) APDB and (100) APDB are produced by deformation of ordered Cu_3Au. Electron microscopy of specimens from stage II showed dislocations to be mostly screw, i.e., suggesting deformation by edge dislocations, and that the majority of these screw dislocations had their connecting APDB apparently lying on (100) planes[14]. To explain these observations, Kear[14] proposed a work hardening mechanism whereby screw dislocations cross-slip on (100) planes to decrease their APDB energy, and are thus pinned. Subsequent deformation occurs at a higher flow stress since the unpinned edge segments must now be bowed out between the pinned screw segments. For an increase in flow stress with increase in strain it is necessary, since the bowing stress is $\sim \frac{Gb}{L}$, that the separation of pinning points, L, decreases with increase in strain. It appears, from a private communication to Davies and Stoloff[21] that Kear has since found little change in L with strain.

Davies and Stoloff[25] suggested that the work hardening rate, at room temperature, of ordered Cu_3Au is similar to that expected for some

f.c.c. metals and alloys; whereas the work hardening rate for the disordered alloy is lower than would be expected. They therefore suggested that work hardening in the ordered material could be explained by the exhaustion of sources caused by dislocation pile-ups at barriers on the primary slip planes, similar to Seeger's work hardening theory[39]. The barriers in the ordered alloy would be due to cross-slip of screws on (100) planes. Davies and Stoloff[27] explained the temperature dependence of the work hardening rate using this model as follows. As the temperature is increased the rate of cross-slip, and hence pinning, increases due to thermal activation. This effect causes an increase in the work hardening rate and a constant yield point with increase of temperature to 350°K. The almost complete absence of stage III in tests at 300°K has been suggested as evidence of strong cross-slip pinning[4]. Above 350°K, Davies and Stoloff suggest, thermal activation is sufficient to cause double cross-slip and, hence, a decrease in the effectiveness of cross-slip pinning, thus explaining the observed decrease in work hardening rate. However, as mentioned earlier, it is felt here that a decrease in the yield stress would indicate a decrease in the effectiveness of cross-slip pinning, but that a decrease in the work hardening rate may correspond to an increase in the yield stress and a decrease in the effectiveness of pinning at higher stresses.

Kear[41] has found no electron microscopical evidence for dislocation pile-ups of the type proposed by Davies and Stoloff.

Vidoz[38] has criticized the cross-slip theories on the grounds that they do not explain why cross-slip on (100) planes should occur,

especially in the early stages of work hardening, which they must do since there is an almost immediate onset of stage II work hardening. He argues that a dislocation on a (111) plane will not 'see' the energy well in (100) planes, but that it will only 'see' the activation energy hill associated with constriction of its stacking fault.

As a result of his recent observation of secondary slip in stage II Kear proposed that the jog mechanism should be a controlling factor in stage II work hardening. He also claimed that the formation of jogs would facilitate the cross-slip of screw dislocations on (100) planes, thus explaining the observed production of (100) APDB, and the proposed cross-slip pinning of screw superdislocations, while overcoming the difficulty, in his earlier model, of the constriction of screw dislocations. Kear frequently observed long screw superdislocation dipoles which, he suggested, were formed by elastic interaction between long cross-slip pinned segments of screw dislocations and new dislocations from the same source. He proposed that these dipoles would annihilate, and form misaligned jogs with associated APDB with increasing frequency as the temperature is increased, thus contributing to the temperature dependence of the work hardening rate. Ham has suggested that other contributions to the temperature dependence of the work hardening rate may be both the temperature dependence of dislocation intersection, and of cross-slip pinning, both of which were discussed earlier.

CHAPTER IV

EXPERIMENTAL TECHNIQUES

1. Specimen Preparation

Lengths of wire (0.040" gauge) of 99.999% purity Au and of 99.999% purity Cu were cleaned in acetone and ether, and weighed out in the proportion 49.1 wt.% Cu (75.5 at.% Cu). These were melted together in an Edwards Speedivac Argon Arc Furnace (Model NS.2139). To minimize impurity pick-up in the alloy during melting, the wires were compacted into a tight ball to reduce their effective surface area, and the copper hearth of the melting unit was cleaned with dilute nitric acid and then acetone. The melting chamber was evacuated, flushed with argon, re-evacuated to a vacuum of 10^{-4} mm Hg, as read on a Pirani-type gauge, and finally filled with argon to a pressure of 400 mm Hg. For several minutes before the alloy was melted, the chamber was Zr gettered. During this process the alloy was protected by a copper cap against the possibility of contamination by evaporated Zr. During melting, the power input was adjusted to keep the maximum amount of the alloy molten and the current required for this purpose was usually 350 amps, and never exceeded 600 amps. To improve the mixing of the constituents, which is retarded at the water-cooled hearth, the button was turned over four or five times and remelted.

Reweighing after melting showed that a 0.05% loss in weight had occurred during melting.

The alloy was hammered and cold rolled from its original button shape, whose approximate dimensions were 1.25" diameter by 0.25" thick, to sheet approximately 0.020" thick. This was then placed in a 1-3/4" Pyrex tube and heated to a temperature of 450°C, while being simultaneously pumped to a fully trapped mercury diffusion pump vacuum of 10^{-5} mm. Hg. The Pyrex was sealed when temperature and vacuum had been attained, and annealing continued for 36 hours.

To examine the efficiency of this homogenizing treatment, specimens were cut from the sheet in directions parallel and perpendicular to the plane of rolling. These were polished to a 1 μ diamond finish, washed, dried, and finally etched for approximately four seconds in the fumes from a freshly mixed solution of 3 parts HCl and 1 part HNO_3. Dendritic segregation, somewhat squashed by rolling, was revealed.

The sheet was then further cold rolled to ∿0.009", and cut into pieces 3/4" x 3/8". These were placed in a silica glass tube, the specimens being separated by 1" diameter A.U.C. graphite discs, and given a further homogenizing treatment of 48 hours in a 10^{-5} mm Hg vacuum at 900°C. To free the graphite spacers of harmful impurities, they had been heated in contact with commercial purity Cu prior to use. The specimens were quenched from temperature by admitting argon to the system and finally by placing the silica glass container in water.

Etching again with aqua regia fumes revealed that the segregation had been removed by this homogenizing treatment.

The material was then given an ordering treatment of 10 days at 380°C (i.e., 8°C below T_c) in a 10^{-5} mm Hg vacuum and slow cooled from 380°C to 150°C at a rate of 10°C per day. The graphite spacers were again used to prevent fusion of specimens.

The specimens were then water quenched, thus breaking the silica glass container, and causing slight surface oxidation. This was easily removed by the electropolishing technique described below. Specimens prior to, and after, electropolishing, are shown in Figs. 7 and 8 respectively.

The grain size of these specimens was determined using a technique involving a count of the number of grains intersecting a randomly orientated line of known length on the specimen surface. The thermal etch, and contrast between grains due to the slight oxide layer, made the annealed specimens suitable for this determination. The specimens were viewed on a Reichert Universal Camera Microscope "Me F" set at a magnification of X59, so that the 11.8 cm. width ground glass viewing screen revealed 2 mm. length of specimen. Defining one count as the number of grains intersected by this 2 mm. length, 150 counts over several specimens were used to determine a typical grain size for this material of $\sim$0.3 mm.

The electropolishing solution used for surface polishing of specimens for fatigue contained 25 gm. CrO_3, 133 ml. glacial acetic acid, and 7 ml. distilled water. A voltage vs. current plot revealed no polishing plateau for this solution, so that slight variation in these quantities resulted in pitting or etching. The current was found to be extremely sensitive to the water content of the solution, so that due to uncertainty

of the water content of the acetic acid, it was found best to start polishing with a solution containing only a few ml. of distilled water and to make further additions, if needed to improve the quality of the polish. The published operating procedure[43] of using 25 volts, a solution temperature of 15 - 20°C and a stainless steel cathode was usually found to give a satisfactory polish. It was found that stirring of the solution during polishing resulted in a poor polish, presumably because it destroyed a viscous polishing layer on the specimen surface.

2. Testing

The testing method finally adopted was rather crude, but it was felt to be acceptable for the purposes of the qualitative analysis undertaken. (An alternative method tried is described in Appendix I.) The apparatus is shown in Fig. 9. It consists of two identical, freely rotating 3/8" diameter brass rods whose axes of rotation are rods positioned on opposite sides of a rigid rectangular frame. A specimen is placed between the rolls and clamped in position to the base. The position of one of the rod axles is fixed, by setting it in clips, while the second axle (and hence roll) is rotated about the first. By reversing this procedure, the reversed bending cycle is described. To prevent damaging the complete surface of the specimen, the rolls were recessed in a position corresponding to the centre of the specimen surface. A rough approximation, using plastic bending theory, a specimen thickness of 0.010", and the roll diameter, gives the surface strain amplitude to be ± 2.5%. This caused failure in ∿60 cycles.

The testing procedure was as follows: in one test, optical photographs and microhardnesses were taken every few cycles to 20 cycles. In another case, microhardnesses and optical photographs were taken every 5 or 10 cycles from 20 cycles until the appearance of the first crack. X-ray intensity measurements were taken from the specimen cycled to failure. Replicas and thin films were taken from these and various other specimens similarly fatigued.

A few tests were carried out at low amplitudes (i.e., an applied stress well above the initial yield stress, but causing failure in a number of cycles greater than 10^6 cycles).

3. Microhardness

Hardness values were taken to determine, on a quantitative basis, the progress of fatigue deformation.

Due to the thickness of the specimens (~0.009"), standard macrohardness equipment could not be used, so that in effect, an attempt has been made to obtain macrohardness values from microhardness measurements.

The Reichert Microhardness Tester with a load of 100 gm. was used, following the recommended procedure. A minimum of ten indentations, both diagonals of each indentation being measured, were used to determine a 'representative' microhardness value. Indentations were made at random within a central area of approximately 1/4" x 1/4", since this was thought to be most representative of the deformation caused by the reverse bending cycling. At greater widths, friction effects, caused by the rolls, were obtained; at the specimen clamps the material was always in tension; while

bending was always stopped short of the other extreme of length to prevent the specimen from springing out from between the rolls. In some cases, this sampling procedure was repeated and found to give hardness values in good agreement with the original ones.

The widths of the slip bands which developed during deformation were small compared to the indentation sizes obtained with a 100 gm. load. The diagonal length of indentations which straddled one or several slip bands appeared to be unaffected by them. Indentation sizes of the order of the slip band width could not be produced, so that a representative hardness value for these regions could not be obtained.

4. Replicas

Single stage replicas were produced by evaporating a 50-50 carbon-platinum film onto the specimen surface using an Edwards Speedivac Coating Unit (Model 12E6/1112) evacuated to 2-3 x 10^{-5} mm Hg, stripping this film off the specimen surface with a coating of parlodion, and finally dissolving the parlodion away with amyl acetate.

It was found that thin evaporated films could not be lifted off the specimen, and in other cases, that they disintegrated in the amyl acetate solution. The latter effect was attributed in some cases to an extreme shadowing effect at large irregularities on the surface. The thickness of the evaporated film could be gauged by the interference colour it produced on the specimen surface and best results were obtained with films which went through the colours to black. For shadowing at a 45° angle, this usually involved evaporating two C-Pt pellets with the specimen 3 - 4 cm. from the pellet in each case. In specimens with large surface

irregularities, it was found necessary to evaporate a 'backing' film of carbon at right angles to, and some 5 - 6 cm. away from, the surface.

The evaporated film was given 3 - 4 coatings of parlodion (dissolved in collodion), one every 3 - 4 hours, and after the final coat, 24 hours were allowed for complete hardening. This coating was then used to strip the evaporated film from the specimen surface. Suitably sized pieces were cut from this sheet and placed, parlodion side down, on 3 mm. diameter, 100 mesh copper electron microscope specimen holder grids. The filter paper holding these grids was then soaked in amyl acetate and a minimum of 12 hours was allowed before the specimens were removed for examination. All replicas were examined in a Siemens Elmiskop I operating at 80 kV, using a non-tilting stage.

5. Thin Films

Thin films were produced by the window technique using the electropolishing solution and the operating condition described for the surface preparation of specimens for fatigue. It was found that the Miccrostop, used to mask off the specimen edges, was attacked by this solution, so that a fine film of Miccrostop spread over the specimen surface during polishing. If polishing was continued under these conditions, the final specimen film was badly pitted, but by removing the Miccrostop masking in the final stages of polishing, pit-free thin films could be obtained. The most even polish was obtained by regularly changing the edge clamped by the electrical lead, so that all edges of the specimen were in turn lower in the solution than the others. To prevent damage to the specimen, the teeth were removed from the alligator clamp electrical connection.

With experience, it was usually possible, using this technique, to obtain at least one film from each specimen which was thin enough for the electron microscope. All thin films were examined in a Siemens Elmiskop I operating at 100 kV, using a double tilt stage.

6. X-ray

A Philips Norelco diffractometer was used to determine the intensity peaks associated with the {100}, {110}, {200}, and {220} reflections from a specimen fatigued to failure, and an electropolished annealed specimen, respectively. Copper radiation (30 kV; 15 ma), a nickel filter, 1° divergence and receiving slits, and a speed of specimen rotation, about an axis perpendicular to its surface, of 100 r.p.m., were used for both specimens. A 1° divergence slit was used since this produced a beam which was contained on the specimen at all angles used. A low scanning speed of 1/8° per minute was employed to increase the efficiency of intensity measurement by the geiger counter. However, the highest counts per second obtained was ∿55 c.p.s., so that counting losses are expected to be small. The low scanning speed employed also resulted in an increase in the area a peak described on the chart, so that the accuracy of measurement of these peaks was increased.

The four peaks were obtained for both sides of both specimens. Each peak was scanned individually, and scanning was started before and continued after the peak, ∿1/2 - 1° in both instances, so that a background level of scattering could be determined. The measurement of peak areas above background was made using a planimeter.

CHAPTER V

RESULTS

1. Surface Observations

a) Optical

The change in slip appearance with increasing number of cycles is shown in Figs. 11 - 15 inclusive. The annealed material is shown in Fig. 8, while the effects of a large tensile deformation and of low strain amplitude fatigue (see Appendix I) are shown in Figs. 10 and 11 respectively. After 1 cycle, slip is fine and general, as in the specimen deformed in tension and that by low strain amplitude fatigue. After 3 cycles, however, dark 'scores' of localized slip are observed, and with increasing number of cycles these become an increasingly predominant feature. Final failure occurred along these slip bands, as shown in Figs. 17 and 18.

b) Replicas

Figs. 19 and 20 show single stage replicas of the surface of the specimen after fatigue. A careful examination of the predominant 'ribbon' feature reveals these to be caused by extrusions. This is perhaps best shown in Fig. 20, where it is seen that the lighter 'protected' areas follow in detail the profile of the dark ribbons, suggesting that these 'ribbons' are due to features raised from the surface. The reverse, of course, could be argued in favour of intrusions, viz., that the dark

regions follow in detail the profile of the light areas. However, the shape of the defect so produced is quite unreasonable.

2. Hardness

The average diagonal length for each of the 10 - 15 indentations made at each of various numbers of cycles are listed in Table I. The students' 't' function was used to determine 95% confidence limits on the readings for each cycle, and the data so obtained, converted to Reichert Microhardness Numbers, is shown in Fig. 21.

It is seen from Fig. 21 that the hardening is rapid in the first 10 - 15 cycles, and then apparently 'saturates'. Correlation of these hardness changes with the corresponding changes in the slip appearance reveals the following: after one cycle at this high strain amplitude, the hardness increased and no localization of slip was observed. After three cycles, localized slip was observed and the hardness had continued to increase. Further cycling caused increased localization of slip with no obvious transition stage which could be associated with the saturation of hardening.

Since the widths of these bands of localized slip were small compared to the hardness indentation, it is suggested that these hardness measurements are more representative of the surrounding regions of general slip. Thus, since the amount of general slip, and hence the change in these hardnesses, decreases with increased localization of slip, 'saturation' is identified with the almost complete localization of slip.

3. Transmission Electron Microscopy

Figs. 22 and 23 show the typical grown-in APDB maze structure. Figs. 24 and 25 show the APDB structure obtained from a specimen fatigued to failure, and it is seen that the domains have been distorted, if not slightly reduced in size, by fatigue. Figs. 26 and 27 show the APDB structure obtained from a specimen fatigued for approximately one-half of its life, viz., 35 cycles. Large amounts of APDB have been produced, and analysis of the diffraction pattern in one case revealed these to be of the {100} type.

Since these specimens were fatigued under the same conditions, the fact that the greatest amount of APDB produced by deformation was observed in the 35-cycle specimen, and not in the one cycled to failure, may at first be surprising. However, attention is drawn to the inhomogeneous nature of this deformation process, as was shown by the surface observation, and the random nature of thinning. For these reasons, it is suggested that the thin film obtained from the 35-cycle specimen is associated with a highly deformed region, possibly a region of localized slip, whereas the thin film obtained from the failed specimen is associated with a region of more general slip.

4. X-ray

The intensity peak areas for the superlattice {100} and {110} reflections, and the fundamental {200} and {220} reflections, from both sides of both an annealed specimen and a specimen fatigued to failure are listed in Table II.

Since superlattice lines are a result of long range order, a measure of the degree of long range order can be obtained by comparing the intensity of these superlattice reflections to the intensity of fundamental reflections. The intensity peak area ratios $\frac{A_{100}}{A_{200}}$ and $\frac{A_{110}}{A_{220}}$ for each side of both specimens are shown in Table III. These ratios were calculated using conjugate reflections to eliminate orientation effects.

The peak areas were reproducible; however, some of the scatter in values may be due to the choice of a level of background scattering, while, as will be discussed later, a greater effect in the annealed specimens is thought to be due to extinction. Large errors in the actual measurement of the chosen peak areas are not expected since each measurement was reproducible.

Theoretical $\frac{A_{100}}{A_{200}}$ and $\frac{A_{110}}{A_{220}}$ intensity peak ratios were calculated for a degree of long range order of unity, from the scattering factor equation for each reflection. There were corrected for changes in intensity due to effects other than changes in the atomic configuration, viz., geometric effects, thermal scattering, and effective atomic size factors (see Appendix II). Comparison of these ratios with those experimentally obtained enabled an estimate of the degree of long range order to be made. These are listed in Table IV.

Values for the long range order parameter of greater than unity, as obtained for the annealed specimens, are suggested to be due to extinction. These high order parameters would then be due to greater extinction of the fundamental reflections than of the superlattice reflections. Such an effect has been previously observed by Mikkola and Cohen[34].

Since this effect could not be corrected for, a true value for the degree of long range order of the annealed specimens was not obtained. However, extinction is not expected to occur in the fatigued specimen, since the mosaic size will have been greatly reduced, so that the order parameters obtained for these specimens are expected to be real.

It is assumed that the order parameter of the annealed specimens, by virtue of their heat treatment, is unity. The long range order parameter of 0.8 - 0.9 obtained for the fatigued specimen would indicate, therefore, a reduction in the degree of long range order by fatigue.

CHAPTER VI

DISCUSSION

The present observation that APDB is produced by deforming ordered Cu_3Au by high strain reverse bending is in agreement with previous examinations of this alloy after deformation by rolling of polycrystals[17], tension of single[14,41] and polycrystals[34,35], and explosive loading of polycrystals[34].

As discussed in Chapter II.6, current work hardening mechanisms for ordered Cu_3Au account for this effect, but are distinguishable by the type of slip-produced APDB which they predict. Flinn[26] predicts ribbons of (111) APDB caused by the jogging of grown-in domains; tubes of (111) APDB lying in a <110> direction are expected from the Vidoz and Brown theory[36]; while (100) APDB is accounted for only by the cross-slip mechanisms proposed by Kear[14,41]. Consequently, the large amounts of (100) APDB seen in the present investigation are consistent with the cross-slip mechanisms suggested by Kear.

In agreement with this observation, large amounts of (100) APDB have been observed to be produced by rolling, tensile testing, and explosive loading of polycrystals of ordered Cu_3Au.

Slip-produced APDB must cause a reduction of the effective domain size, and a reduction of the degree of long range order.

Long range order could also be reduced homogeneously, and it has been suggested that the diffusion of vacancies would give such an effect. However, Nikkola[49] has obtained good agreement with experiment by calculating stored energy values, on the assumption that disordering was due only to the production of APDB by slip, from the amount and type of APDB present after straining. Thus, if Cu_3Au does not disorder homogeneously by deformation, then the APDB energy per unit area of APDB must remain constant during deformation.

Cottrell[31] has calculated the effect of reduction of domain size on strength, assuming the energy of APDB per unit area of APDB (γ) to be constant at all domain sizes. Consider a circular domain of diameter 'ℓ' lying on the slip plane. Prior to deformation the APDB energy per unit area of the slip plane is

$$\frac{4a\gamma}{\ell}$$

where 'a' is the lattice parameter. After deformation has produced APDB over all of the slip plane, the APDB energy per unit area of the slip plane must be γ. Thus equating the change in energy to the work done, $\sigma\ell$, by the applied stress, σ, the following equation for the applied stress is obtained:

$$\sigma = \frac{\gamma}{\ell} - \frac{4a\gamma}{\ell^2} \quad .$$

Differentiation of σ with respect to 'ℓ' shows a maximum applied stress occurs at the domain size of $\ell = 8a$.

While it is felt that this model is too simple to be important quantitatively, it does suggest the important effect that softening should eventually occur by reducing the domain size. This effect is visualized as occurring as follows.

As the domain size decreases, the amount of APDB intersecting the slip plane increases. The amount of APDB on the slip plane prior to deformation has therefore increased, so that the maximum amount of APDB which can be produced by slip on this plane must decrease. Assuming a specific number of active superdislocations, the amount of APDB which each produces must also decrease, resulting in a decrease in the applied stress. This reduction in the amount of APDB that can be produced by slip is only important at small domain sizes. At large domain sizes, the effect of the reduction of the domain size will be to increase the amount of APDB produced by each dislocation, thus increasing the yield strength. Unfortunately it is impossible to test this effect directly since Cu_3Au orders by a process of nucleation and growth, so that small domains co-exist with short range order.

Such an effect was necessitated, as mentioned in Chapter II.6, to reconcile the initial hardening of secondary slip systems, as proposed by Pampillo, with the final softening of these secondary slip systems, as proposed by Vidoz, by increasing the amount of APDB on primary slip planes.

By this argument, the slip appearance of a specimen with an initially large domain size, would be expected to be fine and general, since localization of slip would cause local increase in strength. Should slip reduce the domain size below the critical one, softening, and a resulting localization of slip should occur.

The various aspects of this process have been observed in the present investigation. In the early stages of high strain amplitude fatigue, slip was fine and general, similar to that observed after tensile deformation and low strain amplitude fatigue. This deformation also caused an increase in hardness, so that this and the slip appearance are consistent with strengthening by the production of APDB. However, in contrast to tensile deformation and low strain amplitude fatigue, further cycling led to extensive slip localization, which, judging by the hardness measurements, became complete in the final stages. This localization, in itself, indicates a breakdown in the mechanism of strengthening by the production of APDB. Strong evidence for local softening is afforded by the observed formation of large extrusions in these bands, similar to those associated with fatigue softening materials[48]. These considerations, together with the observation of a gross reduction in the effective domain size suggests a softening effect similar to that proposed by Cottrell.

Extensive localization of slip and associated extrusion formation at grain boundaries was observed recently[5] to occur during the low strain fatigue of β-brass. These effects were attributed to the stress concentration at grain boundaries facilitating cross-slip. By the present argument, the excessive slip activity, associated with stress relief at the grain boundaries, could cause a reduction in the APD size sufficient to assist localization of slip. This argument is consistent with the observation that single crystals of β-brass exhibited a higher fatigue ratio, but that cracks were eventually initiated at regions of slip localization.

The slip bands observed in this present investigation were not restricted to the regions around grain boundaries, although they did appear to be initiated at grain boundaries in many instances. Nor was cracking predominantly intercrystalline as it was in β-brass, although, again, some evidence of this was obtained. For these reasons it appears that the stress concentrations at grain boundaries were not so large in Cu_3Au as they were in β-brass, and it has been suggested[5] that the large elastic anisotropy in β-brass gives rise to this effect.

Recent evidence (reviewed by Ham[44]) suggests that slip bands in low stress amplitude fatigue are caused by localized regions of high stress amplitude, so that the structure created by high stress amplitude tests is indicative of that formed in slip bands in low stress amplitude tests.

Using this argument it is possible to explain the findings of Rudolph et al[4] that the long range order parameter of ordered Cu_3Au was unchanged by fatigue at low stress amplitude.

It should first be explained that no measurable change in the order parameter, as determined by X-ray intensity measurements, does not necessarily indicate that the APD size remains unchanged. From the results of Mikkola and Cohen[34], it is found that reducing the APD size of Cu_3Au, by tensile deformation, from 4320 Å to approximately 800 Å, caused a reduction in the long range order parameter from 1 to 0.98. Further, by explosive loading, it is found that the APD size could be reduced from an original size of 1000 Å to approximately 100 Å with no measureable change in the order parameter.

From the evidence reviewed by Ham, it would be expected that in the specimens of Rudolph et al, regions of slip concentration whose structure is typical of the high stress amplitude structure should form. Thus from the results obtained in the present investigation, these small regions should have a domain size small enough so that, considered by themselves, they would cause a reduction in the degree of long range order. However, the adjacent 'low stress amplitude' areas will not have such a small domain size, and need not, as was shown above, cause a reduction in the degree of long range order. Thus, averaged over the whole specimen, the degree of long range order need not be, and apparently is not, reduced.

Observations on the fatigue behaviour of FeCo and Ni_3Mn have been made by Davies and Stoloff[3]. Ni_3Mn has the same superlattice as Cu_3Au, while FeCo has the same superlattice as β-brass, viz., b.c.c. cell with one species at the corner sites and the other species at the centre sites. It was found that by ordering these alloys, the U.T.S. and the endurance limit were increased an amount such that the fatigue ratios remained constant in both cases. These workers suggest that an increase in U.T.S. on ordering can be attributed to cross-slip pinning. So that they claim in Ni_3Mn, where cross-slip pinning may occur, the U.T.S. is raised; while in FeCo, where cross-slip cannot occur, the U.T.S. will be little affected. Testing these alloys revealed that there was an equivalent increase in the U.T.S. and endurance limit on ordering, such that the fatigue ratio was the same for the ordered and disordered alloys. It was concluded that the propensity for cross-slip pinning also determined the endurance limit. However, it has been suggested[34], on the basis of the negligible temperature dependence of the work hardening rate of Cu_3Au, that cross-slip

pinning, being a temperature dependent mechanism, cannot be an important process in the work hardening of polycrystalline Cu_3Au. Thus we are left with the underlying assumption of the proposal by Davies and Stoloff, viz., that the cause of the strengthening is the same in both fatigue and tensile testing of polycrystalline ordered Cu_3Au. The current theory which appears to explain most of the observations which have been made, is the Vidoz and Brown jog theory. It is of interest to recall that this theory apparently relies on the same effect, of eventual softening with decrease in domain size, as was used to explain the present observations.

CHAPTER VII

CONCLUSIONS

It has been shown that deformation by very high strain reverse bending is initially general, as in tension and low strain amplitude fatigue, but, in contrast to these, finally becomes localized. The large amounts of APDB, which have been shown to be produced, are suggested to give rise to both these effects. This is so, since it is expected that increasing amounts of APDB will initially cause hardening, and finally cause softening of the material. The observed formation of extrusions has been proposed as evidence for localized softening.

CHAPTER VIII

SUGGESTIONS FOR FUTURE WORK

A consequence of an increasing proportion of slip occurring in regions which soften with deformation, must be that the peak stress, to cause constant strain amplitude cycling, decreases. The observation of such fatigue softening in the final stages of high strain amplitude cycling of ordered Cu_3Au would be strong evidence for the mechanism used to explain the present observations. Since the development of a fatigue crack would give a similar effect, caution should be exercised in interpretation of such a drop in peak stress. However, the growth of a fatigue crack, in contrast to a genuine fatigue softening effect, should produce the most marked effect in the tensile peak stress.

An attempt should be made to correlate changes in the surface slip appearance with changes in APD size. A technique of selective thinning would have to be developed for this purpose, and this would have to be, presumably, other than the one attempted in this investigation.

APPENDIX I

EXPERIMENTAL DIFFICULTIES

1. Testing

To produce failure in thin sheets of Cu_3Au by reverse strain proved to be more difficult than anticipated. It was originally intended to utilize the technique developed by Grosskreutz and Waldow[43] for this purpose. These workers bonded thin sheets of Al to the surface of a plexiglass baseplate which was then fatigued in reverse bending, thus inducing tension-compression cycling in the specimen. Their specimens were then removed for thin film electron microscopy by dissolving away the baseplate and adhesive. However, a soluble bonding agent rigid enough to transmit enough strain to cause failure in the Cu_3Au sheets could not be found. Nevertheless, some observations were made which represent the behaviour at low amplitude.

2. Polishing

An attempt was made to utilize the P.T.F.E. polishing technique in conjunction with cyanide, and chromic acid electropolishing solutions respectively. In this technique, polishing has to be stopped at the first appearance of a hole in the specimen, so that the lack of control, in this respect, with these solutions due to the hazardous nature of the former and the opaqueness of the latter, made the technique difficult. Of the two, the chromic acid solution, because of its slower polishing

rate, promised the best results. However, it was found that the P.T.F.E. holder in a chromic acid solution frequently caused edge attack on the 2.3 mm. discs and even when this was overcome, by prior dishing of the discs with an aqua regia jet electropolish, thin films could not be produced.

APPENDIX II

CALCULATION OF THEORETICAL INTENSITY PEAK AREA RATIOS

The theoretical ratio of the intensity of a superlattice reflection to that of a fundamental reflection is given by:

$$\frac{A_s}{A_f} = \frac{S^2[f_{Au}-f_{Cu}]^2}{[3f_{Cu}+f_{Au}]^2} \cdot \frac{\frac{1+\cos^2 2\theta}{\sin\theta \sin 2\theta}}{\frac{1+\cos^2 2\theta}{\sin\theta \sin 2\theta}} \cdot \frac{\frac{\sin(2\theta-\phi)}{\sin\phi + \sin(2\theta-\phi)}}{\frac{\sin(2\theta-\phi)}{\sin\phi + \sin(2\theta-\phi)}} \cdot \exp(+2M) \cdot \exp(+2M') \qquad \text{(Equation II.1)}$$

where

f_{Au}, f_{Cu} = atomic scattering factors for gold and copper respectively,

S = long range order parameter,

θ = Bragg angle

ϕ = incident angle of beam,

$M = 0.52 (\sin \phi/\lambda)^2$,

$M' = 0.22 (\sin \phi/\lambda)^2$,

λ = wavelength of radiation.

The first factor in Equation II.1 is the ratio of the atomic scattering factor equations for intensity. The second, which Taylor[50] calls 'the angular factor', takes into account the change in intensity produced by a change in the angle of reflection. This includes the Lorentz factor, the polarization factor, the probability of reflection factor, and the proportional factor due to the change in size of the

intensity sample. The third factor is for absorption, and since $\phi = \theta$ in the diffractometer, it reduces to 0.5 in the numerator and 0.5 in the denominator, and hence cancels. The penultimate and final factors are thermal scattering, and effective atomic size factors, as given by Borie[46].

The atomic scattering factors were obtained by graphical interpolation of those given in the International Tables[47]. θ was calculated from

$$\sin^2 \theta = \left(\frac{\lambda}{2}\right)^2 \frac{h^2+k^2+l^2}{a^2}$$

using

$\lambda = 1.54221$ Å (Average of Kα wavelengths given by Taylor[50])

$a = 3.744$ Å [42]

Using this method, theoretical ratios at S = 1 of $\frac{A_{100}}{A_{200}} = 0.6518$ and $\frac{A_{110}}{A_{220}} = 1.493$ were obtained.

REFERENCES

1. Avery, D. M., and Backofen, W. A., Fracture of Solids, p.339, eds. D. C. Drucker and J. J. Gilman, Gordon and Breach, New York (1963).

2. Taoka, T., Yasukochi, K., and Honda, R., Mechanical Properties of Intermetallic Compounds, p.192, John Wiley and Sons, New York (1960).

3. Boettner, R. C., Davies, R. G., and Stoloff, N. S., Trans. AIME 236, 131 (1966).

4. Rudolph, G., Haasen, P., Mordike, B. L., and Neuman, P., Paper at Int. Fract. Conf., Sendai, September 1965.

5. Williams, H. D., and Smith, G. C., Phil. Mag. 13, 835 (1966).

6. Bethe, H. A., Proc. Roy. Soc. A150, 552 (1935).

7. Guinier, A., X-ray Diffraction, Dorothée Sainte-Marie Lorrain (1963).

8. Hansen, M., Constitution of Binary Alloys, McGraw-Hill, New York (1958).

9. Ogawa, S., Watanabe, D., Watanabe, H., and Komoda, T., Acta Cryst. 11, 872 (1958).

10. Marcinkowski, M. J., Electron Microscopy and Strength of Crystals, Interscience (1963).

11. Cowley, J. M., Phys. Rev. 77, 669 (1950).

12. Sutcliffe, C. H., and Jaumot, F. E. Jr., Acta Met. 1, 725 (1953).

13. Koehler, J. S. and Seitz, F. J., J. Appl. Mech. 14, A217 (1947).

14. Kear, B. H., Acta Met. 12, 555 (1964).

15. Marcinkowski, M. J., and Miller, D. S., Phil. Mag. 6, 871 (1961).

16. Marcinkowski, M. J., and Zwell, L., Acta Met. 11, 373 (1963).

17. Cohen, J. B., and Bever, M. B., Trans. AIME 218, 155 (1960).

18. Mikkola, D. G., and Cohen, J. B., J. Appl. Phys., 33, 892 (1962).

19. Ardley, G. W., Acta Met. 3, 525 (1955).

20. Fisher, J. C., Acta Met. 2, 9 (1954).

21. Stoloff, N. S. and Davies, R. G., Mechanical Properties of Ordered Alloys, Scientific Laboratory Report, Ford Motor Co., Dearborn, Michigan, 1965.

22. Marcinkowski, M. J., Brown, N., and Fisher, R. M., Acta Met. 9, 129 (1961).

23. Sumino, K., Tohoku University, Sendai, Sci. Repts. of Research Insts., 10A, 283 (1958).

24. Kuczinski, G. S., Doyama, B., and Fine, M. G., J. Appl. Phys. 27, 651 (1956).

25. Davies, R. G., and Stoloff, N. S., Phil. Mag. 9, 349 (1964).

26. Flinn, P. A., Trans. AIME 218, 145 (1960).

27. Davies, R. G., and Stoloff, N. S., Phil. Mag. 12, 297 (1965).

28. Keating, D. T., and Warren, B. E., J. Appl. Phys. 22, 286 (1951).

29. Biggs, W. D., and Broom, T., Phil. Mag. 45, 246 (1954).

30. Davies, R. G., and Stoloff, N. S., Acta Met. 11, 1347 (1963).

31. Cottrell, A. M., Seminar on Relation of Properties of Microstructure, p.151, ASM, Cleveland (1955).

32. Sachs, G., and Weerts, J., Z. Phys. 67, 507 (1931).

33. Hordon, M. J., Trans. AIME, 227, 260 (1963).

34. Mikkola, D. G., and Cohen, J. B., Acta Met. 14, 105 (1966).

35. Kear, B. H., and Wilsdorf, H., Trans. AIME 224, 382 (1962).

36. Vidoz, A. G., and Brown, M. L., Phil. Mag. 7, 1167 (1962).

37. Hirsch, P. B., Phil. Mag. 1, 67 (1962).

38. Vidoz, A. G., Acta Met. 13, 1099 (1965).

39. Seeger, A., Dislocations and Mechanical Properties of Crystals, p.243, John Wiley and Sons, New York (1957).

40. Pampillo, C. A., Phil. Mag. 13, 693 (1966).

41. Kear, B. H., Acta Met. 14, 659 (1966).

42. Annaka, S., J. Phys. Soc. of Japan 9, 354 (1954).

43. Fisher, R. M., and Marcinkowski, M. J., Phil. Mag. 6, 1385 (1961).

44. Ham, R. K., to be published.

45. Grosskreutz, J. C., and Waldow, P., Acta Met. 11, 717 (1963).

46. Borie, B., Acta Cryst., 10, 89 (1957).

47. International Tables for X-ray Crystallography, Vol. III, The Kynoch Press, Birmingham, England (1962).

48. Thompson, N., Adv. in Physics 7, 72 (1958).

49. Mikkola, D. E., Ph.D. Thesis, Northwestern University, June 1964.

50. Taylor, A., X-ray Metallography, John Wiley and Sons, New York (1961).

Number of Indentations	Number of Cycles														
	0	1	3	5	7	9	11	13	17	20	20	30	40	50	60
1	253.5	229.0	206.5	200.0	196.5	177.5	189.0	196.5	186.5	189.5	187.0	193.0	166.0	208.5	191.5
2	253.5	215.0	219.5	197.5	190.5	183.5	190.0	185.5	181.0	184.5	184.0	170.0	198.0	204.0	190.5
3	248.5	221.0	209.0	201.5	189.5	190.0	186.0	203.0	184.5	199.0	182.5	182.0	173.0	185.0	202.0
4	259.0	206.0	201.5	186.0	208.0	195.0	190.5	205.0	190.0	195.5	196.0	184.5	188.0	179.0	189.0
5	251.0	218.5	205.0	197.0	182.0	183.0	170.5	197.5	185.0	192.0	192.5	192.0	194.5	199.5	177.0
6	245.0	230.0	206.0	204.0	191.5	183.5	194.5	196.0	178.0	181.0	200.0	174.5	189.5	186.0	188.5
7	261.0	224.0	216.5	196.5	189.0	164.0	202.0	183.0	178.0	186.5	194.0	178.0	153.0	198.0	199.5
8	239.0	229.5	211.5	204.0	198.0	179.5	198.0	197.0	186.5	191.0	194.5	188.5	168.0	202.0	193.5
9	246.5	227.5	203.5	203.5	205.0	197.0	198.0	193.5	185.0	194.5	193.0	184.5	191.0	195.0	195.0
10	249.5	214.5	205.0	210.0	200.5	198.0	190.0	190.5	176.5	174.0	187.0	192.5	186.0	189.5	196.0
11	263.0	231.5	213.5	193.5	191.5	181.0	185.0	200.0	184.0	196.5	178.0	-	182.5	183.0	202.0
12	249.0	230.5	217.5	195.5	198.5	205.0	176.0	197.5	191.5	185.5	186.5	-	185.5	182.0	185.5
13	-	222.0	-	202.5	186.5	203.5	201.0	190.0	192.5	189.0	191.5	-	-	204.0	177.5
14	-	225.0	-	197.0	195.0	191.5	-	206.0	188.5	176.5	-	-	-	189.0	207.5
15	-	221.0	-	196.5	197.5	207.0	-	187.5	181.0	210.0	-	-	-	-	-

TABLE I: Hardness Indentation Diagonals for Ordered Cu_3Au After Various Numbers of Cycles of High Strain Amplitude Reverse Bending.

	Annealed		Fatigued (to failure)	
	1st side	2nd side	1st side	2nd side
A_{100}	2.13	1.42	3.25	3.21
A_{200}	1.22	0.52	7.145	7.49
A_{110}	2.375	3.16	3.115	3.10
A_{220}	1.195	2.25	2.06	2.90

TABLE II: Area Under Intensity Peaks

	Annealed		Fatigued (to failure)	
	1st side	2nd side	1st side	2nd side
$\frac{A_{100}}{A_{200}}$	1.75	2.73	0.45	0.43
$\frac{A_{110}}{A_{220}}$	1.99	1.70	1.51	1.07

TABLE III: Ratio of Areas Under Intensity Peaks

	Annealed	Fatigued (to failure)
	Average	Average
$\frac{A_{100}}{A_{200}}$	1.85	0.82
$\frac{A_{110}}{A_{220}}$	1.11	0.93

TABLE IV: Calculated Long Range Order Parameter

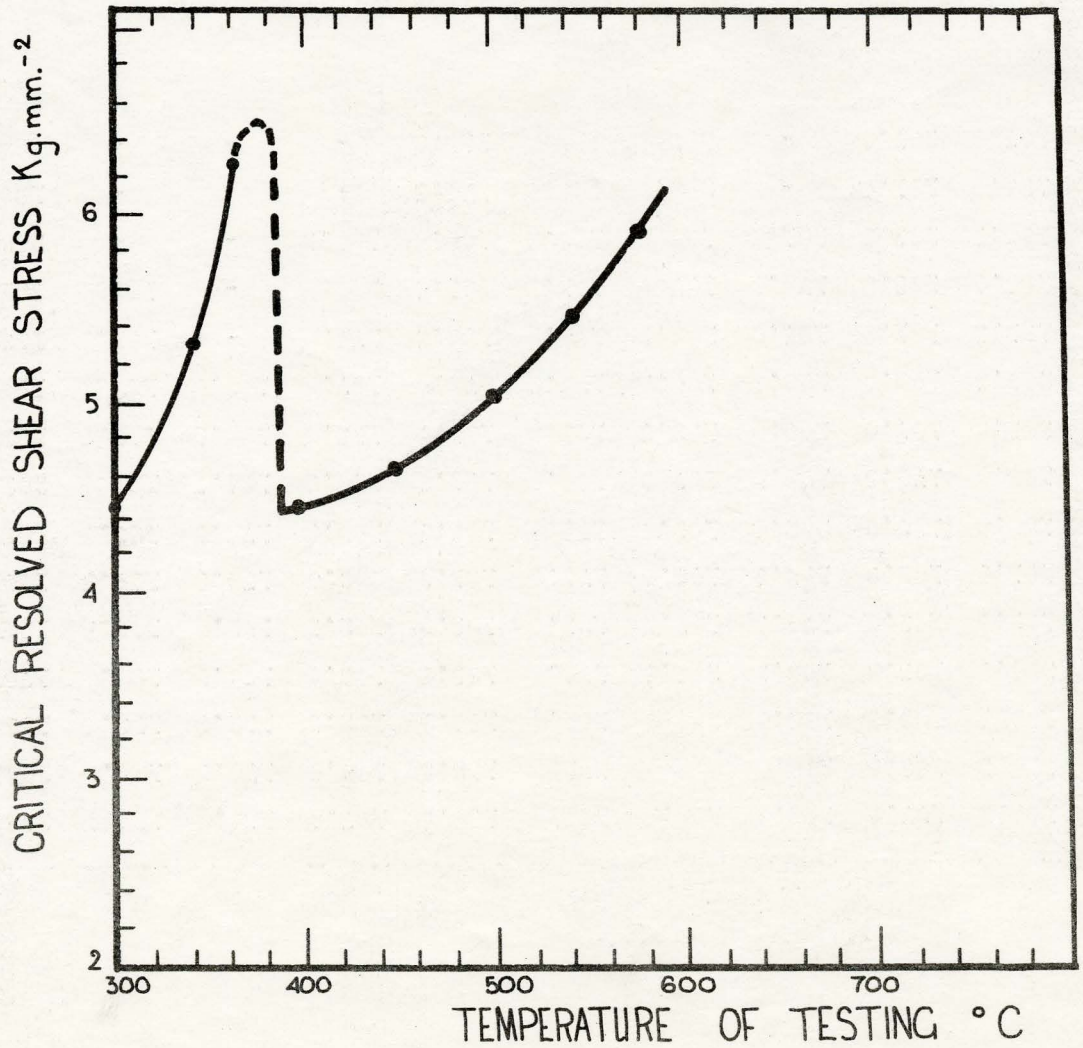

Fig. 1 C.r.s.s. for Cu_3Au Single Crystals Vs. Temperature of Testing (300°C - 600°C) - From Ardley[19]

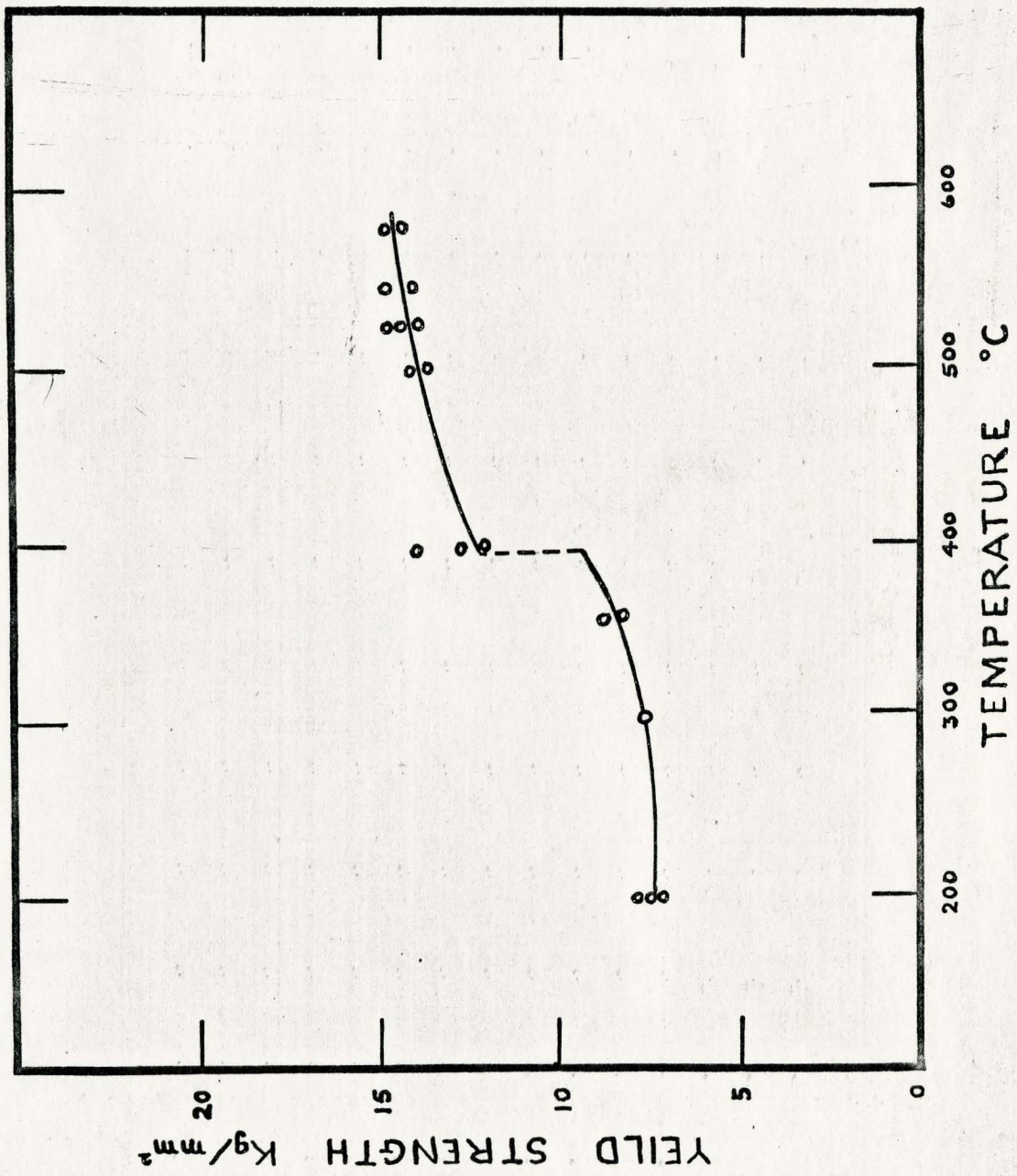

Fig. 2 Yield Strength of Cu_3Au Polycrystalline Wires Vs. Quench Temperature

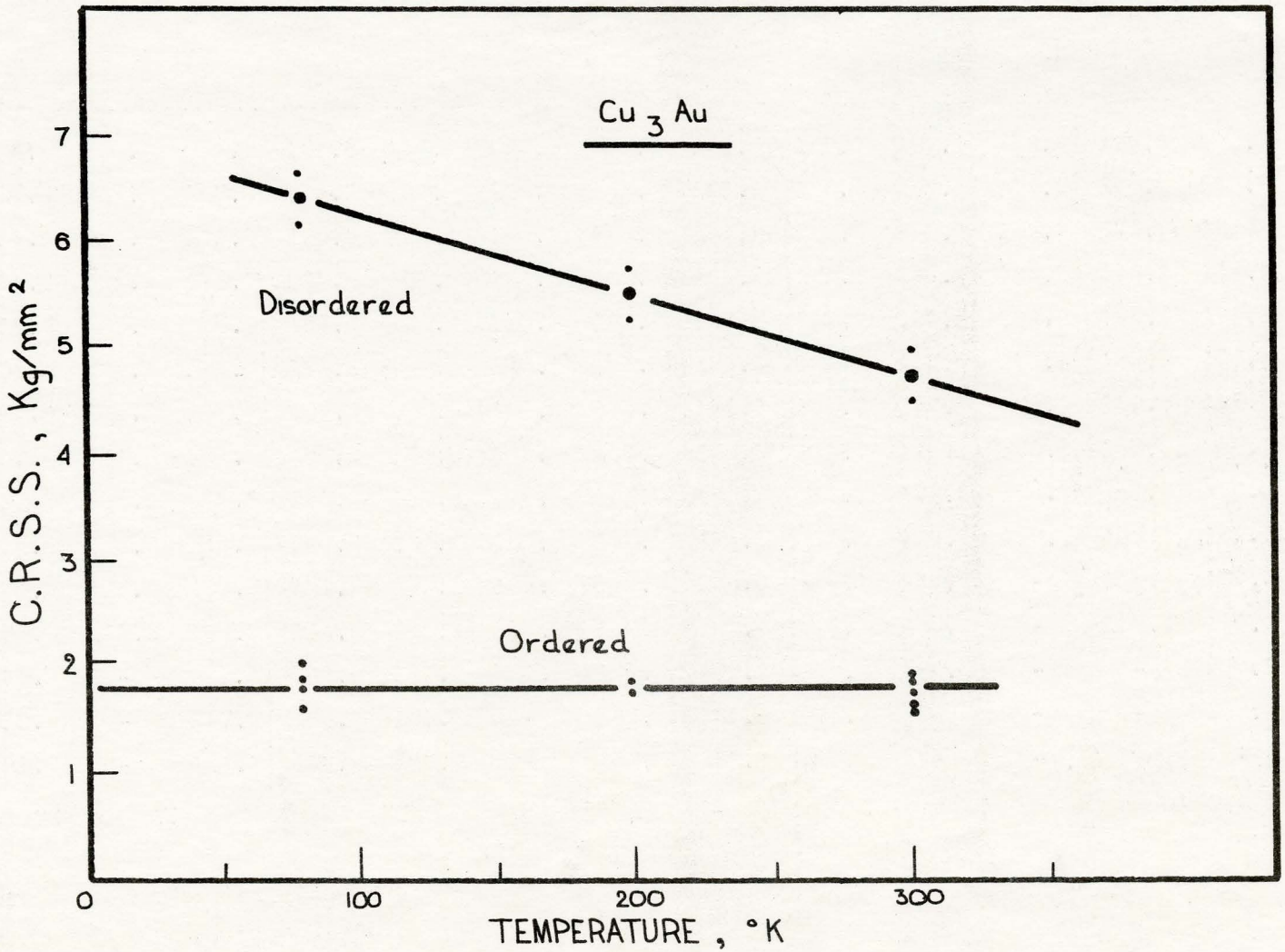

Fig. 3 C.r.s.s. for Cu_3Au Single Crystals Vs. Temperature of Testing (77°K - 300°K) - From Davies and Stoloff[25]

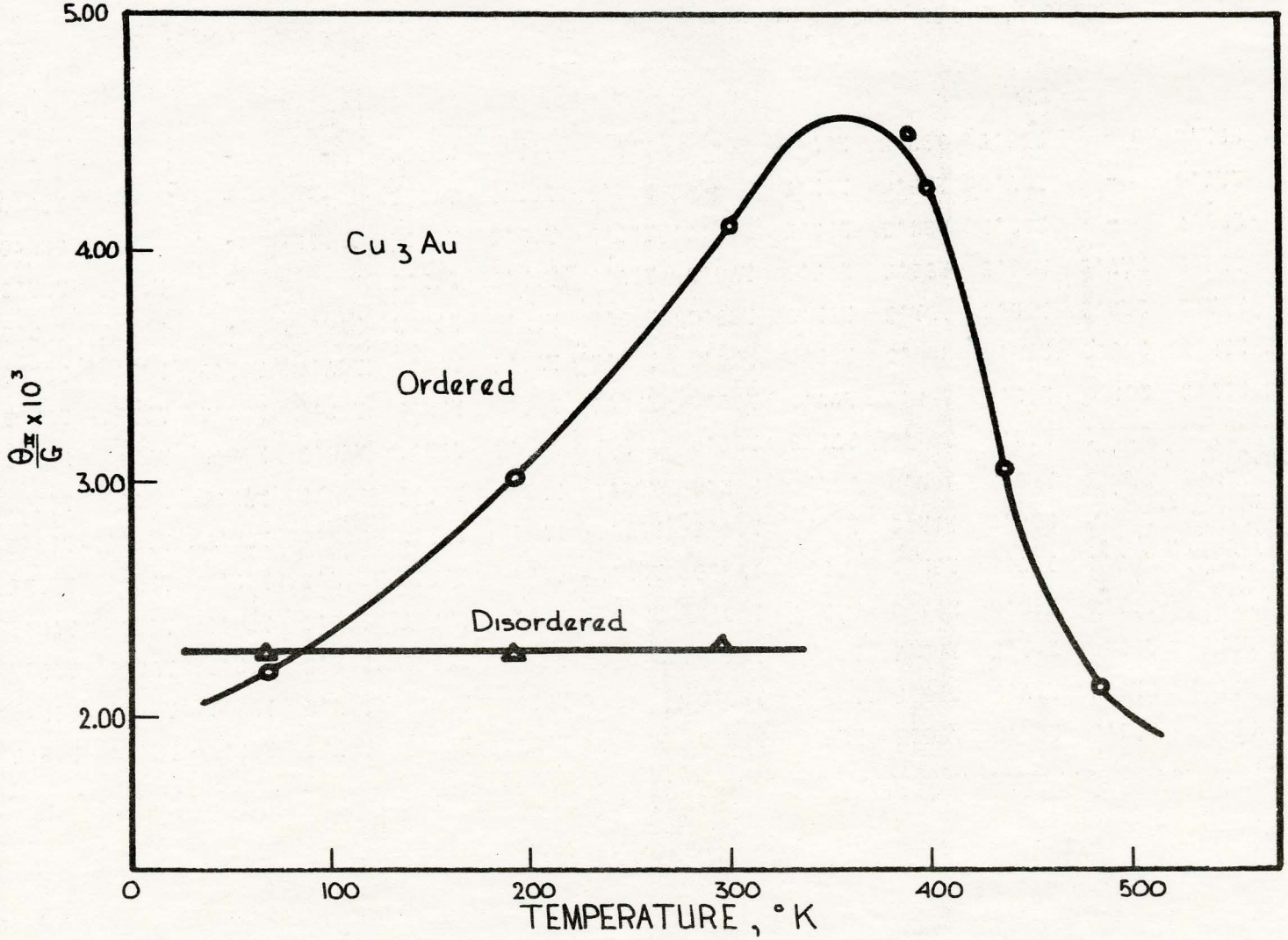

Fig. 4 Stage II Work Hardening Rate for Cu_3Au Vs. Temperature of Testing (77°K - 300°K) - From Davies and Stoloff[25]

Fig. 5 Hardness Vs. Domain Size - From Davies and Stoloff[30]

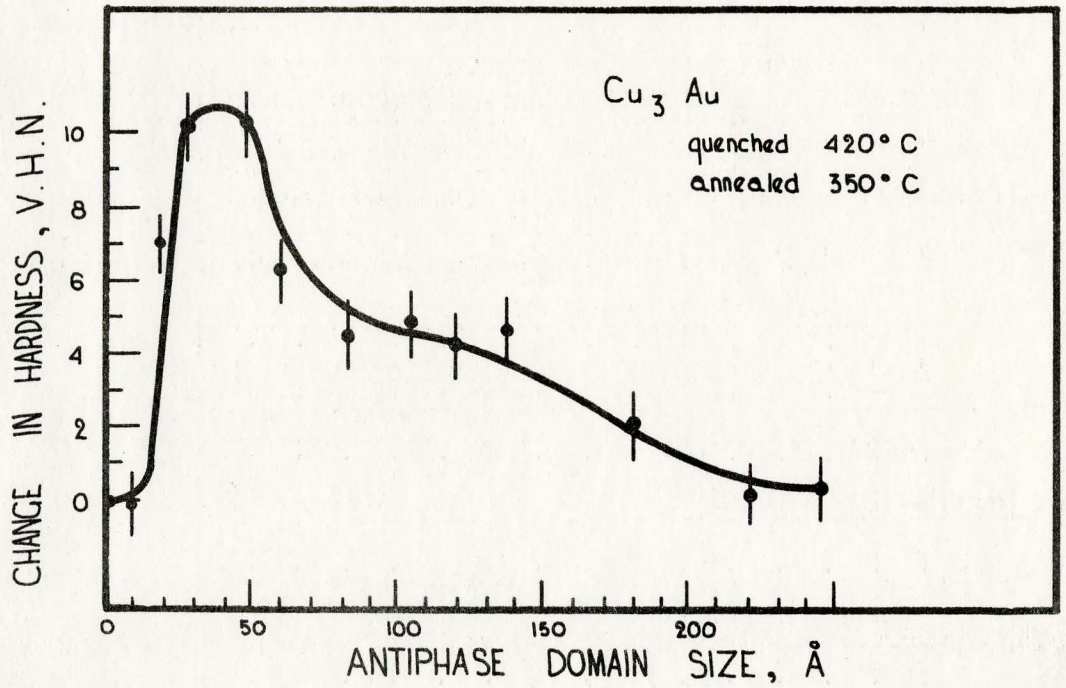

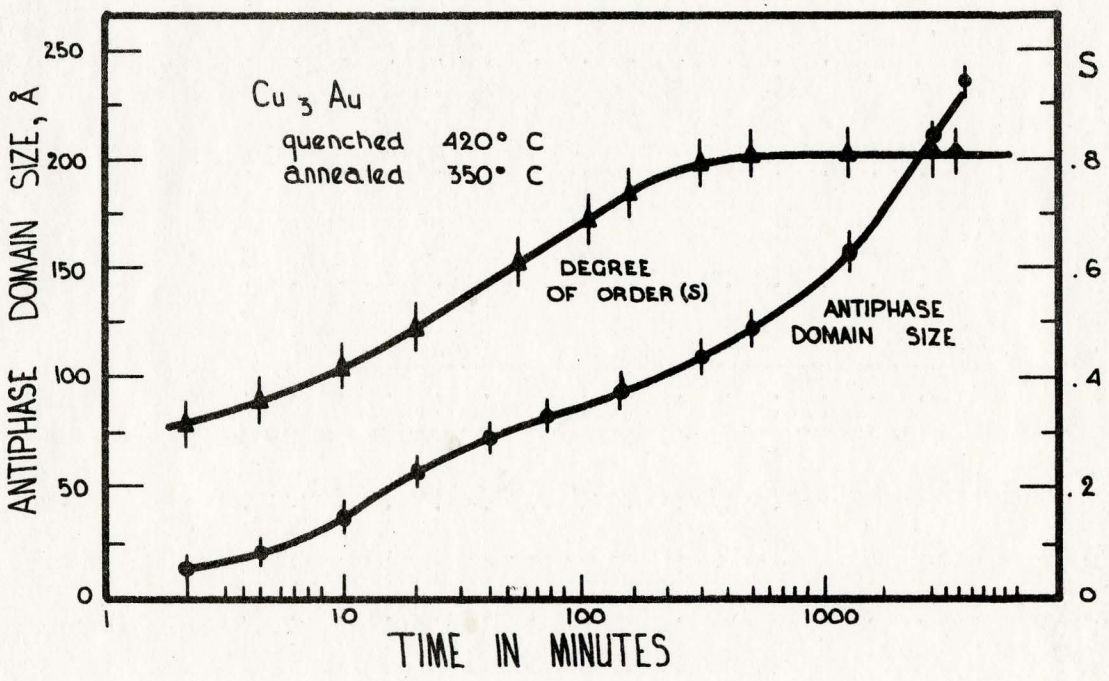

Fig. 6 Degree of Order and Domain Size Vs. Time during an Isothermal Anneal - From Davies and Stoloff[30]

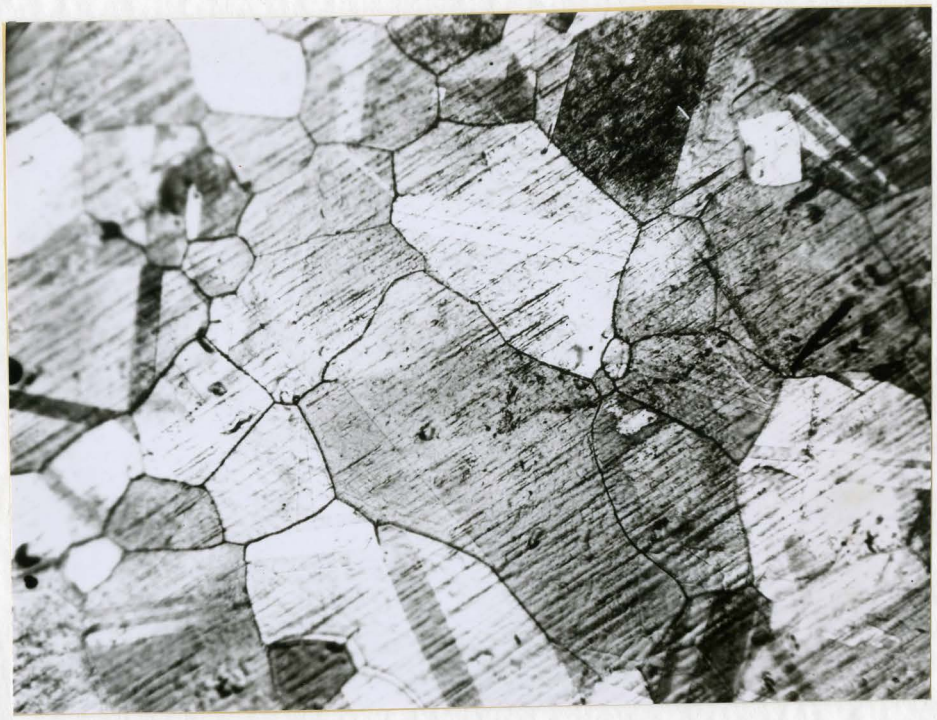

Fig. 7 As annealed ordered Cu_3Au - oxidized. X72.5

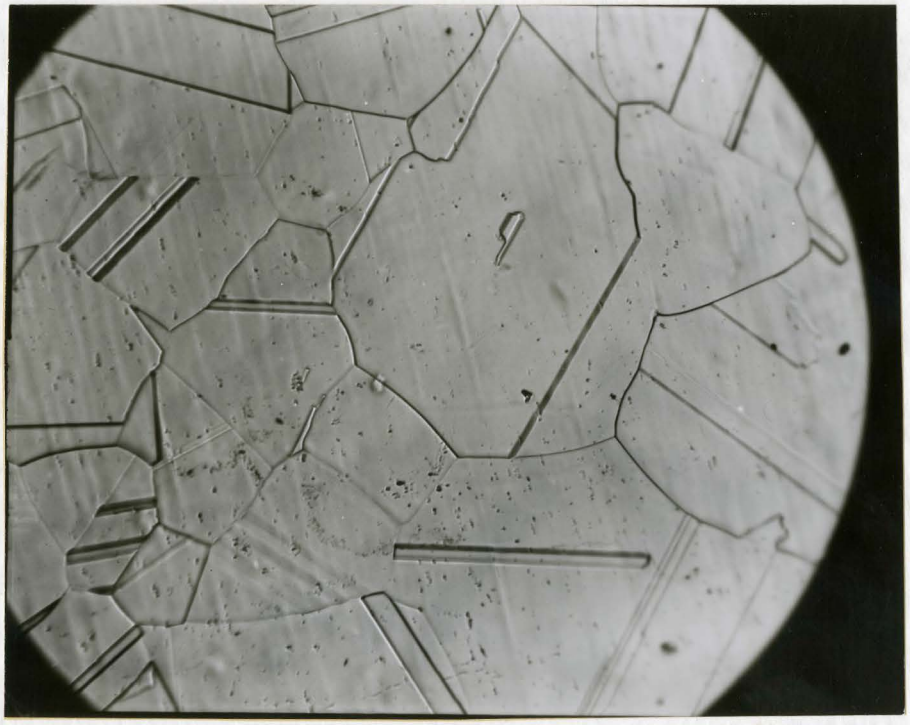

Fig. 8 As annealed ordered Cu_3Au - electropolished. X72.5

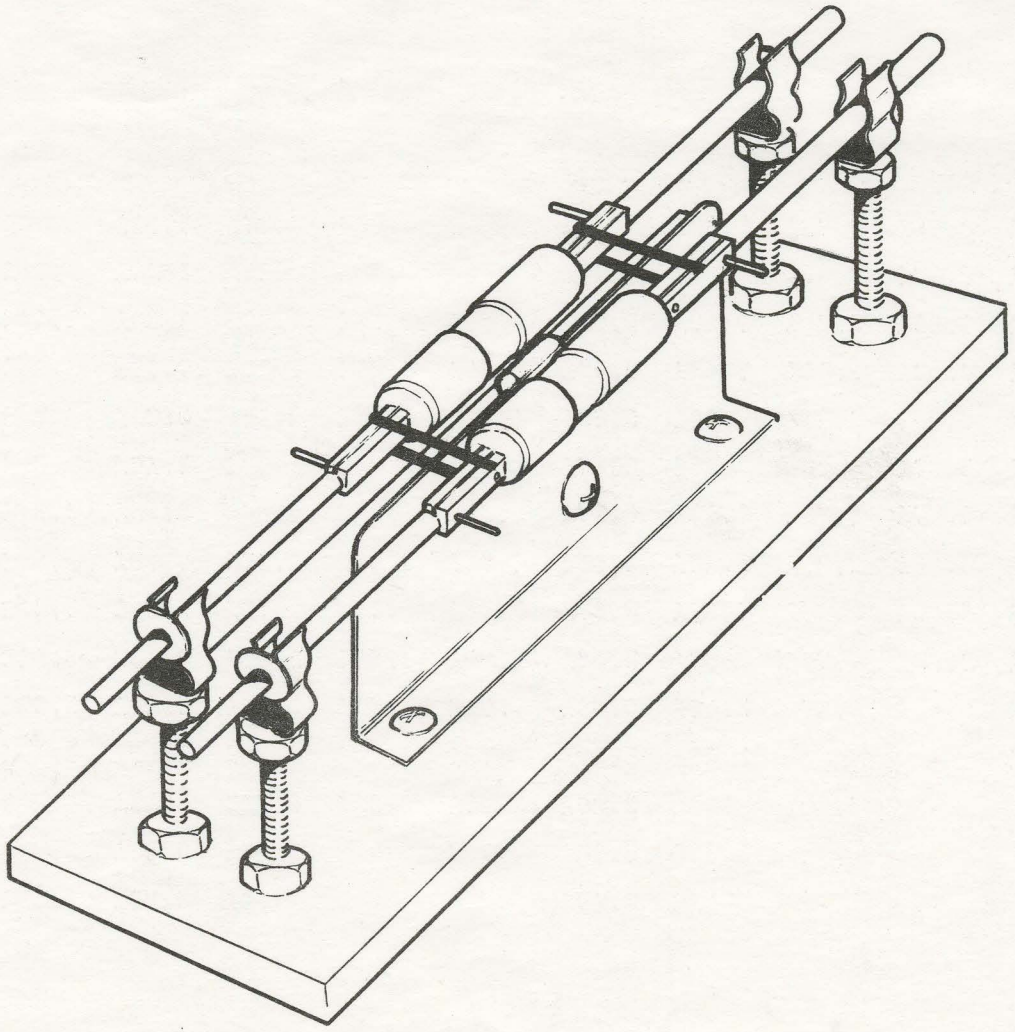

Fig. 9 Reverse Bending Jig

Fig. 10 Ordered Cu_3Au - deformed in tension. X150

Fig. 11 Ordered Cu_3Au - deformed by low strain amplitude fatigue. X150

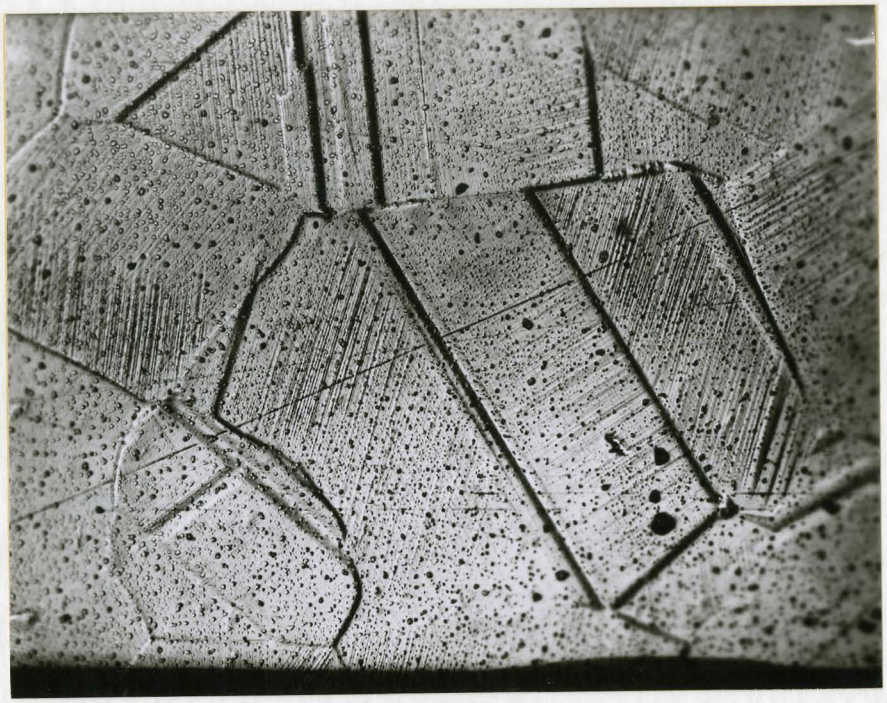

Fig. 12 High strain amplitude reverse bending - 1 cycle. X150

Fig. 13 High strain amplitude reverse bending - 3 cycles. X150

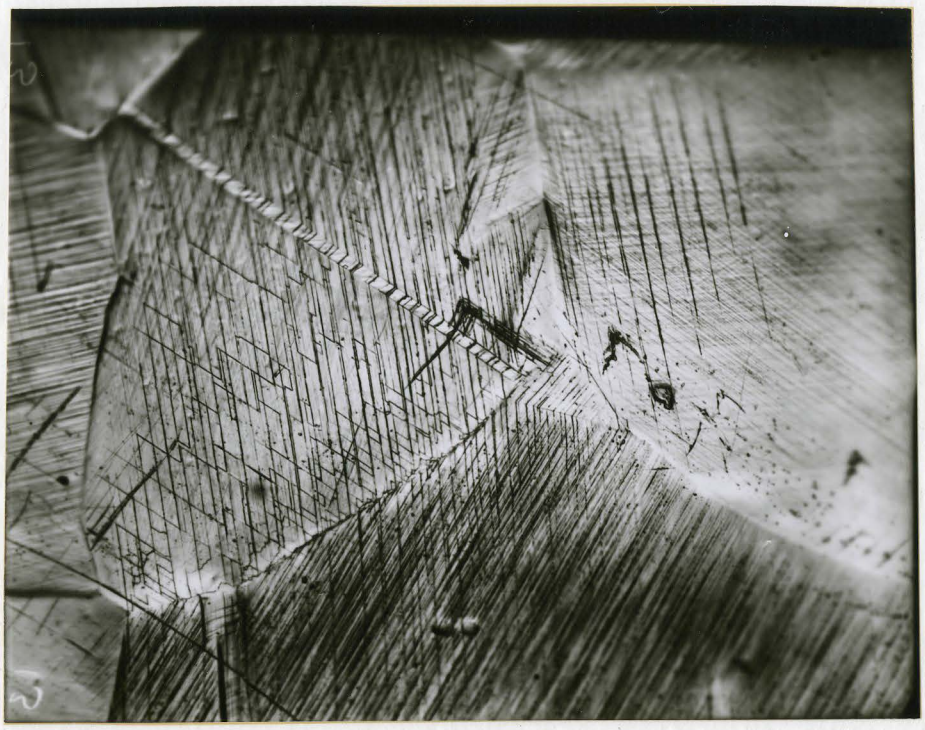

Fig. 14 High strain amplitude reverse bending - 7 cycles. X150

Fig. 15 High strain amplitude reverse bending - 13 cycles. X150

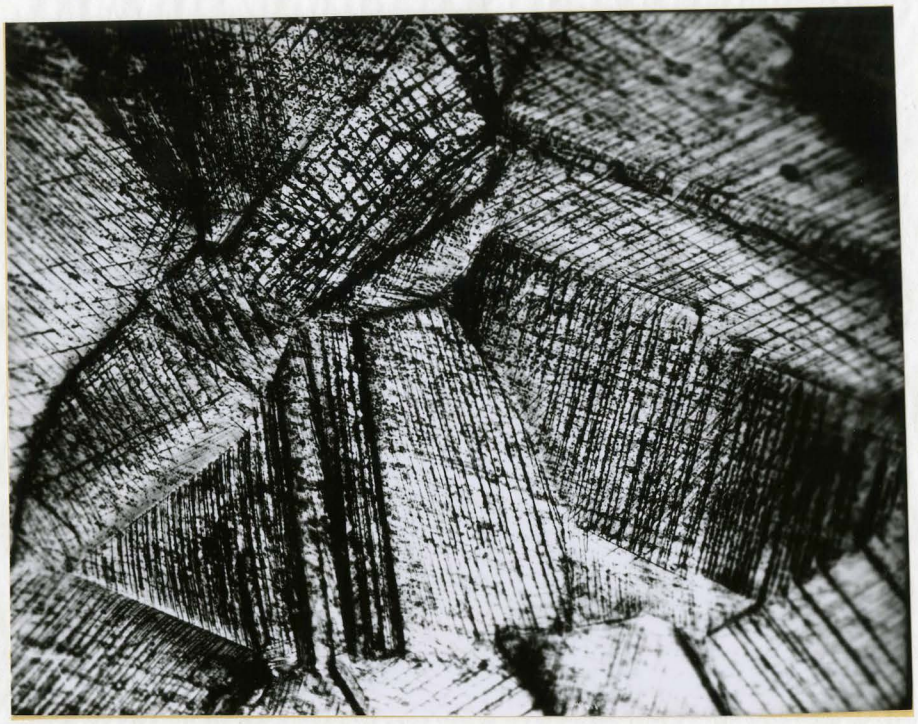

Fig. 16 High strain amplitude reverse bending - 17 cycles. X150

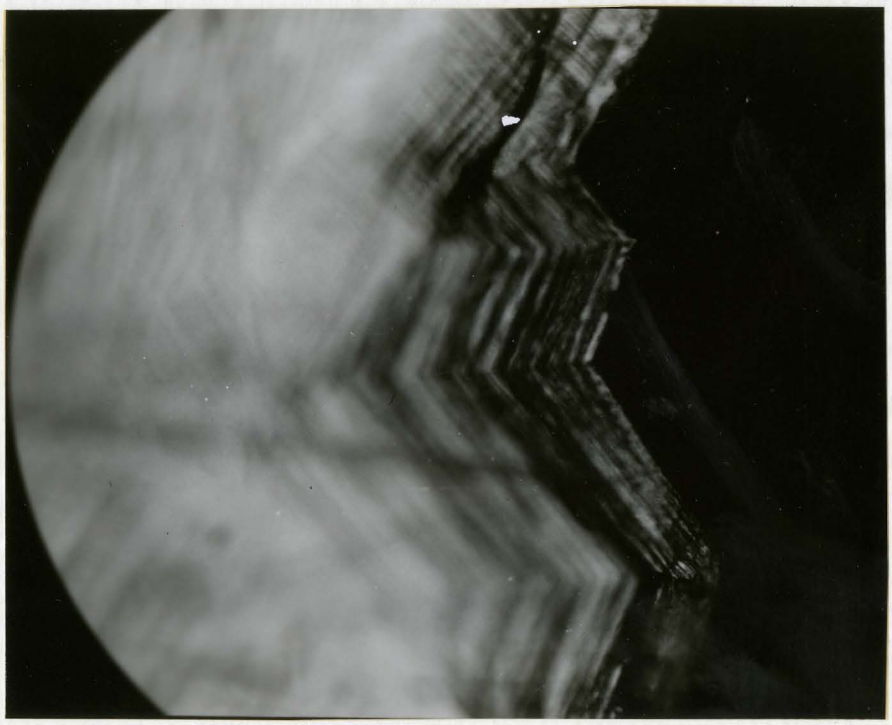

Fig. 17 High strain amplitude reverse bending - failure. X150

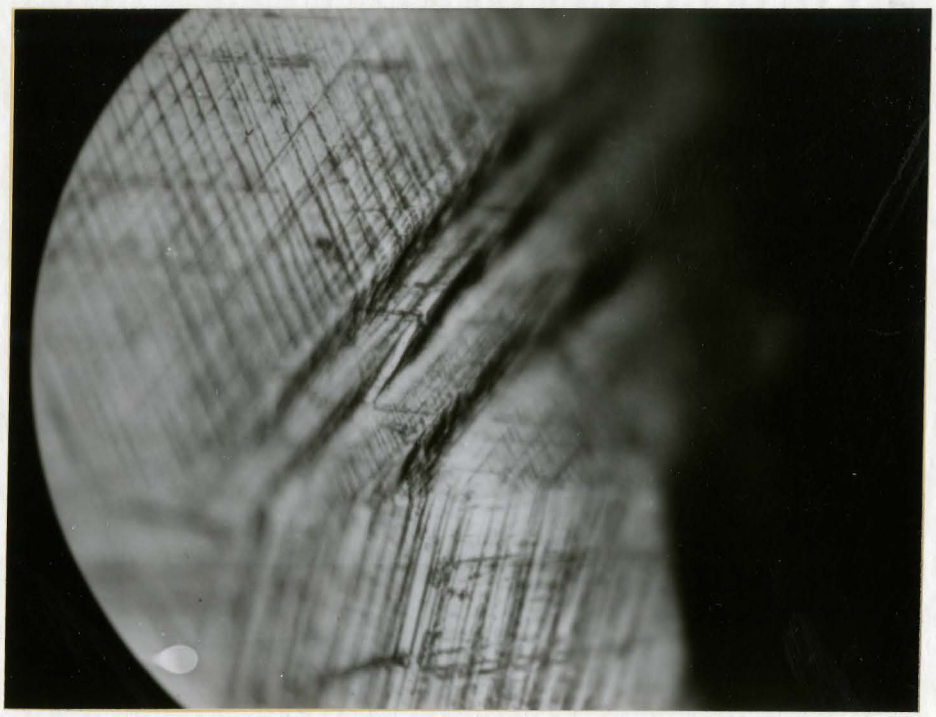

Fig. 18 High strain amplitude reverse bending - failure. X150

Fig. 19 Single stage replica - surface of failed specimen. X5,000

Fig. 20 Single stage replica - surface of failed specimen. X12,000

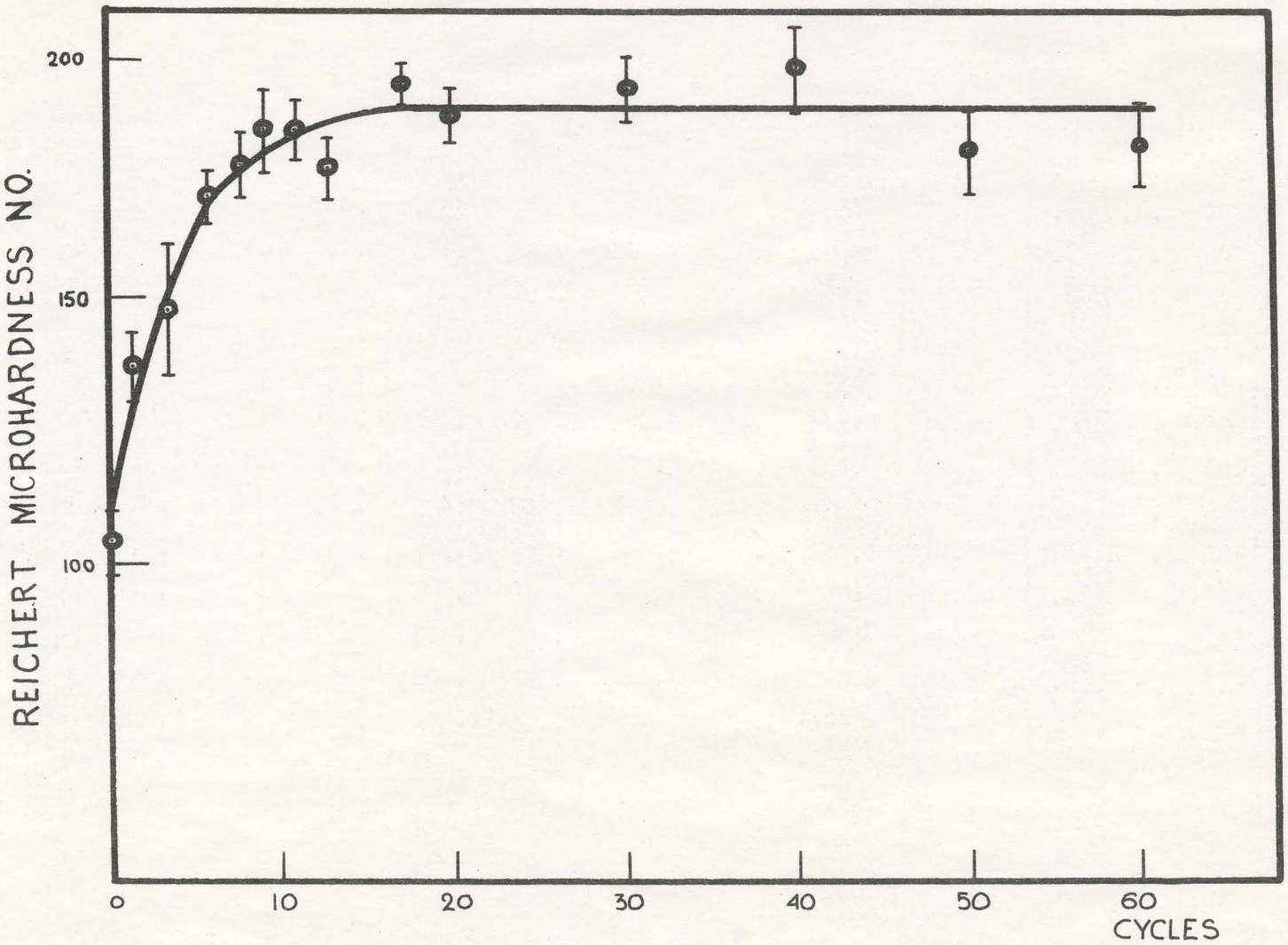

Fig. 21 Reichert Microhardness Vs. Number of Cycles in High Strain Reverse Bending, for Ordered Polycrystalline Cu_3Au

Fig. 22 Electron micrograph of grown-in domain structure. X20,000

Fig. 23 Electron micrograph of grown-in domain structure. X20,000

Fig. 24 Electron micrograph of APDB structure after high strain amplitude cycling to failure. X20,000

Fig. 25 Electron micrograph of APDB structure after high strain amplitude cycling to failure. X20,000

Fig. 26 Electron micrograph of APDB structure after 35 cycles at high strain amplitude. X40,000

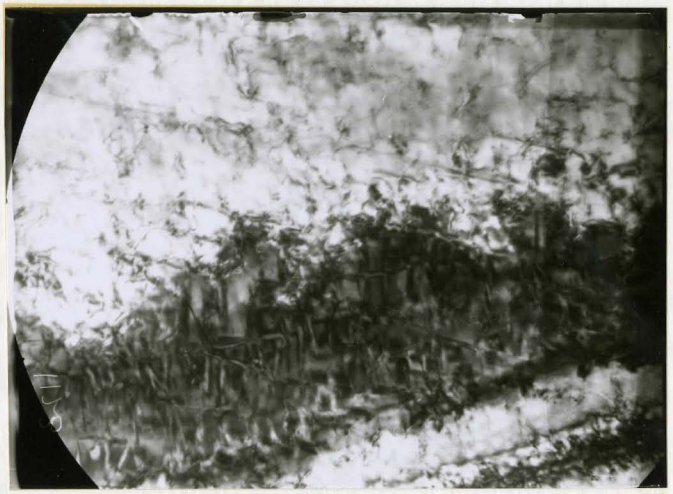

Fig. 27 Electron micrograph of APDB structure after 35 cycles at high strain amplitude. X40,000